First occurrence of the enigmatic peccaries *Mylohyus elmorei* and *Prosthennops serus* from the Appalachians: Latest Hemphillian to Early Blancan of Gray Fossil Site, Tennessee

Evan M. Doughty [Corresp., 1], Steven C. Wallace [2], Blaine W. Schubert [2], Lauren M. Lyon [2, 3]

[1] Department of Ecology and Evolutionary Biology, University of California, Los Angeles, Los Angeles, California, United States

[2] Department of Geosciences and Don Sundquist Center of Excellence in Paleontology, East Tennessee State University, Johnson City, Tennessee, United States

[3] Department of Ecology and Evolutionary Biology, University of Tennessee - Knoxville, Knoxville, Tennessee, United States

Corresponding Author: Evan M. Doughty
Email address: emdoughty@g.ucla.edu

Two peccary species, *Mylohyus elmorei* and *Prosthennops serus* are described from the medium-bodied fauna of the Gray Fossil Site (GFS) of northeastern Tennessee. This site, recognized as an oak-hickory forest, is latest Hemphillian or earliest Blancan based on mammalian biochronology, with an estimated age of 4.9-4.5 Ma. The GFS represents the only site outside the Palmetto Fauna of Florida with *M. elmorei*, greatly expanding the species range north over 920 km, well into the Appalachian region. This is also the first Appalachian occurrence of the relatively widespread *P. serus*. Our understanding of intraspecific variation for both *M. elmorei* and *P. serus* is expanded due to morphological and proportional differences found in cranial and dental material from the GFS, Tyner Farm locality, Palmetto Fauna, and within the literature. The GFS *M. elmorei* material represents the most complete mandible and second cranium for the species, and preserve intraspecific variation in the length of the diastema, dental proportions, and the complexity of the cuspules hypoconulid complex. Similarly, mandibular material from the GFS for *P. serus* exhibited larger dentitions and a greater degree of robustness than currently recognized for the species.

1 **First occurrence of the enigmatic peccaries *Mylohyus elmorei* and *Prosthennops serus* from**

2 **the Appalachians: Latest Hemphillian to Early Blancan of Gray Fossil Site, Tennessee**

3 Evan M. Doughty[1], Steven C. Wallace[2], Blaine W. Schubert[2], and Lauren M. Lyon[2,3]

4 [1]Department of Ecology and Evolutionary Biology, University of California - Los Angeles, Los

5 Angeles, California United States

6 [2]Department of Geosciences and Don Sundquist Center of Excellence in Paleontology, East

7 Tennessee State University, Johnson City, Tennessee United States

8 [3]Department of Ecology and Evolutionary Biology, University of Tennessee - Knoxville,

9 Knoxville, Tennessee United States

12 Corresponding Author: Evan Doughty

13 103 Hershey Hall, 612 Charles E. Young Drive East

14 Los Angeles, CA 90095-7246, United States

15 Email address: emdoughty@g.ucla.edu

First occurrence of the enigmatic peccaries *Mylohyus elmorei* and *Prosthennops serus* from the Appalachians: Latest Hemphillian to Early Blancan of Gray Fossil Site, Tennessee

Evan M. Doughty[1], Steven C. Wallace[2], Blaine W. Schubert[2], and Lauren M. Lyon[2,3]

[1]Department of Ecology and Evolutionary Biology, University of California - Los Angeles, Los Angeles, California United States

[2]Department of Geosciences and Don Sundquist Center of Excellence in Paleontology, East Tennessee State University, Johnson City, Tennessee United States

[3]Department of Ecology and Evolutionary Biology, University of Tennessee - Knoxville, Knoxville, Tennessee United States

Abstract

Two peccary species, *Mylohyus elmorei* and *Prosthennops serus* are described from the medium-bodied fauna of the Gray Fossil Site (GFS) of northeastern Tennessee. This site, recognized as an oak-hickory forest, is latest Hemphillian or earliest Blancan based on mammalian biochronology, with an estimated age of 4.9-4.5 Ma. The GFS represents the only site outside the Palmetto Fauna of Florida with *M. elmorei*, greatly expanding the species range north over 920 km, well into the Appalachian region. This is also the first Appalachian occurrence of the relatively widespread *P. serus*. Our understanding of intraspecific variation for both *M. elmorei* and *P. serus* is expanded due to morphological and proportional differences found in cranial and dental material from the GFS, Tyner Farm locality, Palmetto Fauna, and within the literature. The GFS *M. elmorei* material represents the most complete mandible and second cranium for the species, and preserve intraspecific variation in the length of the diastema, dental proportions, and the complexity of the cuspules hypoconulid complex. Similarly,

43   mandibular material from the GFS for *P. serus* exhibited larger dentitions and a greater degree of

44   robustness than currently recognized for the species.

45   **Introduction**

46   Tayassuidae, a family of pig-like artiodactyls endemic to the New World, is

47   geographically and temporally widespread (Wright, 1998). East of the Mississippi River,

48   however, late Hemphillian to early Blancan faunas are rare. The Palmetto Fauna of Florida is

49   similar in age to Gray Fossil Site (GFS), and is represented by an aggregation of multiple mine

50   localities (e.g. Fort Green Mine, Palmetto Mine, Payne Creek, Saddle Creek Mine, and South

51   Pierce quarries) within the Central Florida Phosphate District of Polk, Hillsborough, Manatee,

52   and Hardee counties (Fig. 1) (Wright & Webb, 1984; Wright, 1989; Hulbert, 2001; Webb et al.,

53   2008). Outside of the Palmetto Fauna, the eastern record is represented by the Pipe Creek

54   paleosinkhole of Indiana (Hh4) (Farlow et al., 2001; Prothero & Sheets, 2013), the Mauville

55   local fauna of Alabama (Hh2) (Hulbert & Whitmore, 2006), and the Tyner Farm locality of

56   Florida (late Hh1 to early Hh2) (Hulbert & Whitmore, 2006; Hulbert et al., 2009a). Specifically,

57   the Tyner Farm and Mauville local faunas both chiefly exhibit *Prosthennops serus* (Hulbert &

58   Whitmore, 2006; Hulbert et al., 2009a) whereas the Pipe Creek fauna is attributed by Prothero

59   and Sheets (2013) to include *Protherohyus brachydontus* (=*Catagonus brachydontus*; see Parisi

60   Dutra et al., 2017**)** and *Platygonus pollenae*. Tayassuids are also identified within the fauna

61   present at the Gray Fossil Site (GFS), with Parmelee et al. (2002) suggesting cf. *Protherohyus*

62   sp. However, based on the fragmentary nature of the material recovered at that time, subsequent

63   workers identified GFS peccaries to the family level only (e.g., Wallace & Wang, 2004;

64   DeSantis & Wallace, 2008).

65   The GFS, located in eastern Tennessee (Fig. 1), is one of the few localities in the eastern

66   United States that represents the latest Hemphillian (Hh4) to earliest Blancan (Wallace & Wang,

67   2004; Samuels, Bredehoeft & Wallace, 2018). An oak-hickory forest surrounded the

68   approximately 2.6-3.5 ha lacustrine deposit, which has a maximum depth of 42m; the GFS is

69   comprised of up to eleven paleosinkholes within the Cambrian to Ordovician dolostone of the

70   Knox Group (Shunk, Driese & Clark, 2006; Whitelaw et al., 2008). For a full review of the

71   geology of GFS see Shunk, Driese & Clark (2006) and Shunk et al. (2009). Early descriptions

72   from the GFS constrain the site to 7 to 4.5 Ma, based on the presence of *Teleoceras* and

73   *Plionarctos*, but a recent description of *Gulo sandorus* from the site included a list of additional

74   fauna which suggest an lower age limit of approximately 4.9 Ma (Wallace & Wang, 2004;

75   Samuels, Bredehoeft & Wallace, 2018). This diverse fauna and flora from this site appears to

76   suggest that the oak-hickory forest surrounding the lacustrine system was a refugium for

77   otherwise disappearing taxa due to the spread of grasslands throughout other regions of the

78   United States (Wallace & Wang, 2004; DeSantis & Wallace, 2008). Despite bearing taxa with

79   Asiatic affinities (e.g., Wallace & Wang, 2004; Liu & Jacques, 2010; Ochoa et al., 2012)—much

80   of the fauna of the GFS exhibits great similarity to that of the Palmetto Fauna of Florida (Hulbert

81   et al., 2009b; Bourque & Schubert, 2015). This includes *Tapirus polkensis*, *Teleoceras* sp.,

82   *Plionarctos* sp., and *Alligator* sp. (Wallace & Wang, 2004; Webb et al., 2008; Short, 2013).

83   These similarities extend to the previously unstudied GFS peccary material and the multiple

84   tayassuid taxa recognized within the Palmetto Fauna (Wright & Webb, 1984; Wright, 1989,

85   1998; Hulbert et al., 2009a).

86   Considering the above, analysis of the GFS tayassuid material provides a unique

87   opportunity to better understand the latest Hemphillian to earliest Blancan of the Appalachian

88   region and its relation to other similarly aged sites within eastern North America. Here we report

89   the first occurrence of *Mylohyus elmorei* outside the Palmetto Fauna of Florida, recognize

90   *Prosthennops serus* within Appalachia, and discuss the implications of multiple tayassuid

91   specimens occurring at the GFS and the region. Additional tayassuid material is recognized

92   within GFS, however, more work is required to verify a full designation.

93   **Methods and Materials**

94   Linear measurements (mm) follow Von den Driesch (1976), whereas nomenclature

95   regarding skeletal morphology follows Woodburne (1968), Sisson and Grossman (1975), and

96   Wright (1989, 1991, 1998) (Fig. 2). Dental measurements and nomenclature were adapted from

97   Wright and Webb (1984) and Wright (1991) (Fig. 3). Images of specimens within the University

98   of Florida Museum of Natural History collections were taken with a Nikon d5100 camera using a

99   Nikon AF-S Micro-NIKKOR 60mm f/2.8G ED lens and are available on the FLMNH website—

100 www.flmnh.ufl.edu/vertpaleo-search/—through NSF grant CSBR 1203222 (Sean Moran, pers.

101 comms., 2015). GFS specimens were photographed using a Canon EOS Rebel Xsi camera and

102 tripod or MK DigitalDirect Photo-eBox Plus Digital Lighting System.   All images were edited

103 using GIMP 2.0, Inkscape 0.91, and Adobe Photoshop CS2 and CS5.

104 **Specimen Repositories—ETMNH,** East Tennessee State University Museum of Natural

105 History—Fossil Collections, Gray, Tennessee; **ETVP**, East Tennessee State University Museum

106 of Natural History—Comparative Collection, Johnson City, Tennessee; **UF**, Division of

107 Vertebrate Paleontology, Florida Museum of Natural History, University of Florida, Gainesville,

108 Florida; **UF/TRO**, Timberlane Research Organization, Lake Wales, Florida (part of the John

109 Waldrop Collection now housed at the Division of Vertebrate Paleontology, Florida Museum of

110 Natural History, Gainesville, Florida).

111   **RESULTS**

112   **Systematic Paleontology**

113   Class MAMMALIA Linneaeus, 1758

114   Order ARTIODACTYLA Owen, 1848

115   Family TAYASSUIDAE Palmer, 1897

116   Subfamily TAYASSUINAE Palmer, 1897

117   Genus *Mylohyus* Cope, 1889

118   *Mylohyus elmorei* (White, 1942) Wright & Webb, 1984

119   **Holotype**—MCZ 3805: partial L. ramus with p2-m3.

120   **Referred Specimens**—ETMNH 7279: L. M2 with partial maxilla; ETMNH 8046: reconstructed

121   partial maxilla with L. and R. P2-M3, partial mandible with L. p3-m3 and R. p2- m3; ETMNH

122   17219: partial L. p3; ETMNH 19281: L. m2; UF/TRO 440, UF 203540: isolated R. M3.

123   Additional referred specimens listed by White (1942) and Wright and Webb (1984) (Table S1).

124   **Description—** Cranium of ETMNH 8046 exhibits a partial maxilla with the left portion of the

125   laterally convex rostrum extending from the P2 to the anterior margin of the canine buttress (Fig.

126   4). Buttress exhibits an irregular shape; bearing both triangular and hemispherical outlines in

127   dorsal and lateral views, respectively. A deep, anteroventrally tapering concavity separates the

128   buttress and the rest of the rostrum. Concavity is bordered laterally by a thin anteromedial to

129   posterolaterally oriented crest that increases in robustness posterodorsally until merger with the

130   dorsal apex of the buttress. Occlusal surface of the anterior buttress is comprised of a triangular

131   patch of relatively flat cortical bone that is separated from the bulbous, inflated lateral margins of

132   the buttress by a shallow ridge. Left canine alveolus is intact and ellipsoid in outline but canine

133   is not present. Post-canine diastema between the posterior boundary of the canine alveoli and P2

134   is long—approximately 110% of total cheek tooth series length (Table 1)—and contains a

135   shallow diastemal crest that trends its full length. Rostrum exhibits a laterally extending crest

136   along the dorsal surface that is the origination of pneumatic zygoma. Crest is bulbous and

137   inflated along its anterodorsal margin whereas the inferior boundary is marked by

138   posteroventrally trending curvature of the maxillary bone. No internal structure of this portion of

139   the zygoma is preserved; however, a deep sinuous depression is present posteromedial of the

140   crest. A shallow to moderate supraorbital sulci trends the length of the dorsolateral surface of

141   the rostrum, originating posteromedial to the lateral crest and terminating anterior and dorsal of

142   the left canine buttress. Ventral surface of rostrum exhibits a palatine sulcus that extends medial

143   of the P2 to the canine buttresses. The remaining medial portion of the palate posterior of the P2

144   is reconstructed with the posterior portion of the sulci lacking. Maxillopalatine region along the

145   dorsal surface of the palate is sinuous. Within the maxillopalatine labyrinth, the thin—

146   approximately 1.52mm width—nasal septum diverges approximately 7.5 mm anterior of the P2.

147   Internal surface of maxilla dorsal and anterior of the P2 appears to exhibit thin, shallow

148   anteroposteriorly trending sulci. Nasal passage is incomplete with the medially projecting

149   remnants indicating a posteriorly constricting tubular profile that trends posterodorsally from

150   medial of the canine buttress to medial of the origination of the zygoma, dorsal to the chambers

151   of the maxillopalatine labyrinth. Vomeroethmoid chamber is directly ventral of the nasal

152   passage and lateral of the nasal septum. Lateral expansion of the chamber is evident posterior of

153   the canine buttresses due the lateral bulging of the cortical bone of the maxilla, with the external

154   surface being convex whereas the interior surface is comprised of a moderate elliptical

155   depression. Medial surface of the rostral cortical bone is pockmarked by numerous intersecting

156   sulci of very shallow depths. Further analysis of the maxillopalatine labyrinth as described by

157   Wright (1991) is not possible due to the lack of preservation.

158   Mandible of ETMNH 8046 exhibits an elongate, gracile condition and is mostly complete

159   but lacking the anterior margin of the symphysis, right mandibular condyle, and right coronoid

160   process (Fig. 5). Canine alveoli and the anterior margin of symphysis are missing. Despite being

161   incomplete, the symphysis is relatively gracile and elongate with a moderate to deep, medially

162   positioned spout-like concavity along its anteroposterior length that bears similarities with the

163   mandibular spout present in ground sloths (e.g. Mcdonald and De Muizon, (2002), De Muizon et

164   al., (2003)). This mandibular concavity is laterally bounded by raised ridges that trend

165   posteriorly and then dorsoposteriorly until the base of the p2. A single mental foramen is evident

166   ventral to the trigon of the p4 on the labial surface of the right rami.   Two genial pits are

167   positioned within a shallow laterally trending genial fossa along the posterior surface of the

168   symphysis medial to the rami. A shallow transverse ridge trends along the ventral-most edge of

169   the symphasis ventral to the genial fossa. Distance between anterior edge of the p2 to the

170   posterior edge of the symphysis is ~43.5 mm. Rami are mediolaterally gracile with a relatively

171   consistent depth along the cheek tooth series, however, the region in contact with the cheek teeth

172   is medially inflated relative to the ventral margin of the rami (Table 2). Ventral surface of the

173   rami retains a relatively similar width leading to the development of a shallow digastric fossa and

174   submandibular fossa between the p2 and m3 which opens posteriorly into the shallow pterygoid

175   fossa. Ventral to the m3, the left mandibular foramen, despite being damaged, appears to be

176   ellipsoid in profile as it opens into a moderate to shallow, anteroposteriorly trending mylohyoid

177   groove. A small mental foramen is positioned ventral to the anterior cusps of the p4 along the

178   labial surface of the right rami. Coronoid process exhibits a triangular outline with a shallow to

179   moderately deep masseteric fossa. Angle originates approximately ventral to the posterior

180   margin of the m3 and exhibits a shallow pterygoid fossa that is bounded posteroventrally by a

181   shallow ridge.

182   Specimen (ETMNH 8046) exhibits moderate wear on the teeth of the upper and lower

183   dentition (Fig. 6 and Fig. 7). Premolars of the lower and upper dentition exhibit a mostly

184   quadrate, molariform condition with moderate anterior and posterior cingula. Exhibiting a more

185   squared to trapezoidal outline, the P2 bears a longer labial edge relative the lingual edge due to a

186   strong, lingually terminating anterior cingulum along the anterior surface of paracone (Table 1).

187   Paracone and anterior cingulum are merging through wear on the right P2 along the anterolingual

188   moiety of the cusp. However, this merger is incomplete as a shallow furrow still separates the

189   median to lingual moiety of the cusp. Trigon and talon are separated by a moderate to deep

190   median valley. Metacone is conic in outline with the left P2 exhibiting slight merger of the cusp

191   with the posterior cingulum along the posterolignual-most edge of the cusp; a shallow furrow

192   separates the posterior edge of the cusp from the cingulum. Hypocone is worn to merger with

193   the posterior cingulum which reduces labially until its termination along the posterolabial to

194   labial edge of the metacone. An ellipsoid fossette is visible on the anterior moiety of the

195   hypocone on the left P2.

196   Third and fourth upper premolars of ETMNH 8046 exhibit similar morphology except for

197   the latter being slightly larger. Both exhibit a merger of the protocone and the weak anterior

198   cingulum through wear. Protocone is merging anterolabially with the heavily worn paraconule is

199   whereas the paracone remains separated from either feature by a moderate furrow. Metaconule

200   and hypoconule are positioned anteromedial and posteromedial to the hypocone and metacone,

201   respectively. Both metaconule and hypoconule merge with the hypocone through wear.

202   Ellipsoid to semilunar fossettes are located at the center of the metaconule, hypoconule, and

203   hypocone. Metacone is separated from the remainder of the talon by a very shallow furrow.

204   Posterior cingulum is moderate, trending the entire posterior edge of all but the left P3 which

205   exhibits chipping of the enamel posterior to the metacone. A depression is evident along the

206   posterior cingulum of the left P4 and the anterior cingulum of the M1, which may represent a

207   cavity or pathology.

208   Upper molars of ETMNH 7279 and ETMNH 8046 exhibit typical tayassuid morphology

209   due to the square to rhombohedral placement of the four primary cusps and strong to moderate

210   anterior and posterior cingula. Left M1 exhibits a continuation of the depression of the P4 at the

211   site of paraconule on the anterior cingulum. Paraconules on both the M1 and M2 (of both

212   ETMNH 7279 and ETMNH 8046) are merging with the paracone through wear, whereas the M3

213   only exhibits merger of the paraconule with the anterior cingulum. All molars exhibit labial

214   cingula that are weak to moderate along the anterolateral edge of the paracone, within the deep

215   median valleys between the labial cusps, and along the posterolateral surface of the metacone. A

216   single accessory cuspule populates the labial cingulum within the median valley of the M2 and

217   M3, however, the cuspule in the latter is reduced. Both the trigon and talon have been almost

218   completely worn into irregularly-shaped, transversely elongate fossettes in the M1. Talon

219   fossette exhibits a partially separation of the metacone fossette from the rest of talon fossette by a

220   thin remnant of lingual to posteriorly bounding enamel (right) or raised dentin (left) that opens

221   anterolingually. Alternatively, the M2 only exhibits merger of the hypocone and metacone with

222   the hypoconule and the metaconule, respectively. Metaconule is heavily worn in the M3 but

223   remains separated from the metacone and hypocone by shallow furrows. In the M2 the

224   hypoconule is worn flat with the posterior cingulum and is merging with the hypocone. Posterior

225   cingulum is strongly developed and bears a small accessory cuspule at its termination at the

226   posterolabial edge of the metacone. Four distinct cusps and conules are present on the

227   moderately worn hypoconulid complex of the M3 in addition to the hypoconulid. Three of these

228   accessory cuspules are arranged in a transverse row along the posterior boundary of the complex

229   and are merging through wear. The remaining cuspule is positioned directly labial to the

230   hypoconule. Posterior cingulum is reduced to a small but strong shelf positioned posterolingual

231   of the metacone and dominated by two small accessory cuspulids.

232   Lower premolars of ETMNH 8046 exhibit similar morphology to the upper premolars;

233   however, the p2 is more transversely constricted (Table 2). In total, each premolar displays a

234   fully formed protoconid, metaconid, hypoconid, and entoconid. Protoconid and metaconid of the

235   p2 are distinct, but not fully bifurcated as in the p3—in both ETMNH 8046 and ETMNH

236   17219—and the p4. Anterior cingula are variable between premolars, being weakly developed

237   but become inflated at the site of the paraconulid in the p3 and p4. Metacone of the p3 and p4

238   exhibits an ellipsoid to rectangular posterolabial extension that is distinct from the parent cusp in

239   ETMNH 17219. Premolar talonid basins exhibit a metaconulid and hypoconulid that are

240   positioned directly anteromedial and posteromedial of the entoconid and hypoconid,

241   respectively, in a 'cross-'or 'plus-' shaped configuration. Posterior cingulum exhibits additional

242   crenulation and very small accessory cuspules on the p4 that are not present on the p3. A slight

243   elevation of the trigonid cusps, relative to the talonid cusps, is evident in ETMNH 17219

244   whereas ETMNH 8046 lacks this feature due to a greater degree of wear.

245   Heavily worn, the m1 of ETMNH 8046 exhibits complete obliteration of all cusps and

246   conules. Trigonid and the anterior cingulum are worn to a single transversely trending fossette.

247   Wear of the talonid produces an ellipsoid fossette with ellipsoid extensions into the positions of

248 the entoconulid and hypoconulid. Trigonid and talonid fossettes are separated from one another

249 by a thin band of enamel on the right m1. However, the left m1 exhibits merger of the trigonid

250 and talonid fossettes in tandem with the posterior cingulum almost being completely worn.

251 Moderately deep, semispherical concavities are present within the dentin at the positions of the

252 metaconid and entoconid of the right m1 and the posterior margin of the posterior cingulum of

253 the left m1 indicating a potential pathology.

254   Similar to the m1 in general outline and apparent cusp arrangement, the m2 and m3 are

255 less worn. Anterior cingulum is moderate to strong in both ETMNH 8046 and ETMNH 19281.

256 Angular wear facets along the surface of the protoconid and metaconid merge the cusps

257 anteriorly with the anterior cingulum. Both cusps exhibit a central fossette along the occlusal

258 surface, with the protoconid exhibiting an anterolabial extension of the fossette into the median

259 of the anterior cingulum. Posterolateral projection of the metaconid is merged with the main

260 body of the metaconid through wear in both ETMNH 8046 and ETMNH 19281. Hypoconid is

261 separate from the hypoconulid in ETMNH 19281, but is merged through wear in ETMNH 8046.

262 Hypoconulid is separate in both specimens, however, it is merged with the strong posterior

263 cingulum through wear in ETMNH 8046. Despite being slightly less worn, the m3 exhibits a

264 similar positioning of the primary cusps as the m2 with the presence of a hypoconulid complex.

265 Four distinct cusps or conulids, including the hypoconulid, are positioned on the hypoconulid

266 complex of the right m3; whereas the left m3 exhibits five conules in ETMNH 8046. On both

267 m3's the hypoconulid is positioned posteromedian of the talonid with the accessory cuspules, of

268 variable size and profile, being positioned posterior to the hypoconulid in a circular arrangement.

269 **Comparisons**—Material from the GFS is referred to *Mylohyus* due to the presence of distinct

270 apomorphies; specifically, a long diastema that exceeds the length of the cheek tooth row and

271 fully molarized premolars (Wright, 1991, 1998). This material is referred to *M. elmorei* on the

272 grounds that it bears notable similarity to material previously collected from the Palmetto fauna

273 of Florida (Table S1). Dental morphologies of ETMNH 8046 and a cast of the holotype, MCZ

274 3805 (labeled UF 57280), display very few differences outside of the latter exhibiting relatively

275 larger dental dimensions for all but the p4. This is due to the holotype having less robust

276 cingula—both anterior and posterior—on the p4 than that of ETMNH 8046. A concave

277 depression on the lingual surface of the m1 metaconid is also evident in the holotype cast. Other

278 potential differences may be obscured due to the p3 missing its talonid on the holotype.

279 Alternatively, the p3 of UF/TRO 412 displays variation of the talonid: with the entoconulid and

280 hypoconulid being merged into a single anteroposterior trending rectangular cuspule that is

281 positioned median of the entoconid and hypoconid. Distinct posterolabial extensions of the

282 metaconid on the p3 and p4 are only present in UF/TRO 412, UF 293749, and UF 57280.

283 Moderate wear obscures the number of accessory cuspules present on the posterior cingula of the

284 p4 in ETMNH 8046, UF/TRO 412, and UF 57280. Five accessory cuspules of variable size are

285 visible on the posterior cingulum of the p4 on UF 294729. Hypoconulid complex exhibits a

286 substantial amount of variation between the observed specimens. Three cuspules (including the

287 hypoconulid) are evident on UF/TRO 412, whereas UF 57280 and ETMNH 8046 exhibit

288 hypoconulid complexes comprised of four and five, respectively.

289   Dental and cranial morphologies are relatively similar between ETMNH 8046 and UF

290 12265. Both ETMNH 8046 and UF 12265 exhibit a very elongate post canine diastema, the

291 former being ~109% of the cheek tooth row, whereas the latter exhibits a diastema of only

292 ~101% (Fig. 8). Origination of the triangular zygoma is positioned directly dorsal to the P2 in

293 both specimens; however, further comparisons are not possible due to the fragmentary nature of

294   ETMNH 8046. Little deviation outside of tooth dimensions of the P2-M2 is present between

295   ETMNH 8046 and UF 12265. Consequently, the M3 exhibits a greater degree of variation with

296   ETMNH 8046 exhibiting a wider talon and hypoconule complex, relative to the trigon, than

297   those of UF 12265, UF 203540, and UF/TRO 440. Further differences between the specimens

298   are evident in the lateral flaring of the canine buttress in UF 12265 that is not present in ETMNH

299   8046 (Fig. 9). Specifically, the flaring in UF 12265 begins on the approximate anteroposterior

300   midpoint of the postcanine diastema, whereas the buttresses flare develops within the anterior-

301   most portion of the postcanine diastema in ETMNH 8046. These dental and cranial differences

302   could be indicative of these specimens representing different species; however, this seems

303   premature because the GFS specimen will be the second partial cranium reported for the species.

304   As such, the variation (geographic, temporal, sexual, or individual) present within the species is

305   unknown, however comparisons could be made to known degree of intraspecific variation in

306   *Mylohyus fossilis* and extant species to show that this range of variation is more likely

307   intraspecific rather than interspecific.

308   cf. *Mylohyus elmorei* (White, 1942) Wright & Webb, 1984

309   **Referred Specimens—**ETMNH 6767: partial L. zygoma and maxillary fossa.

310   **Description—** Highly sinuous cortical bone is evident in both the proximal and distal

311   reconstructions of the left zygomatic wing, ETMNH 6767. Comprised of three associated

312   portions of a left zygomatic wing, ETMNH 6767 exhibits the squamosal portion of zygoma with

313   an intact mandibular fossa. A lambdoid crest of moderate depth projects posterodorsally from

314   the confluence of the zygomatic wing and jugal bar. Ventrolaterally oriented, the semilunar

315   mandibular fossa is positioned posterior and ventral to the zygoma, with the concave-most

316   margin of the fossa being approximately equal in level with the zygoma. Zygoma remnants

317 exhibit a triangular dorsal outline of the posterior margin where the inflated portion reduces

318 posterodorsally to a thin edge. Deeply incised cortical bone demarcates the partial, circular to

319 ellipsoid, rostral muscle fossa on the ventral surface of the reconstructed segments of the main

320 distal body of the zygoma. Another muscle attachment is evident along the flat dorsal surface of

321 this distal section in the form of an anteromedially trending muscle scar, comprised of an

322 elongate raised ridge. It should be noted that both ETMNH 6767 and ETMNH 8046 could

323 potentially be a single individual, however, given the spatial distribution of the two specimens

324 they are considered separate for this analysis.

325 **Comparisons**—Despite being comprised of reconstructed fragments, ETMNH 6767 appears to

326 exhibit affinities to UF 12265 due to the mandibular fossa being positioned posterior and ventral

327 to the posterior margin of the triangular zygomatic wing. This separates ETMNH 6767 from

328 either *Protherohyus brachydontus* and *Prosthennops serus*, which exhibit a mandibular fossa that

329 is positioned directly ventral of the trailing edge of the wing-like zygoma. Moreover, the

330 anterolateral to posteromedial angle of the posterior margin of ETMNH 6767 further mirrors UF

331 122665. Conclusive assignment of ETMNH 6767 is withheld as a larger and less fragmentary

332 sample of *M. elmorei* is needed for a reliable taxonomic assignment.

333 Genus *Prosthennops* Gidley, 1904

334 *Prosthennops serus* (Cope, 1877) Gidley, 1904

335 **Holotype**—AMNH 8511: partial mandible with R. i1,2, p2-m1 and L. i1-3, p2-m3.

336 **Referred Specimens**—ETMNH 410: isolated L. p4; ETMNH 5615: partial mandible with L.

337 and R. i1-m3; UF/TRO 413: L. m2-m3; UF 220251: L. m3. Additional referred specimens listed

338 in Hulbert et al. (2009a) and Schultz and Martin (1975) (Table S1).

339   **Description**—As a partial mandible, ETMNH 5615 (Fig. 10) is lacking the coronoid, condylar,

340   and angular processes. Mandibular symphysis is long with the dorsal surface exhibiting a

341   moderately deep spout-like concavity with a posteroventral orientation. This mandibular

342   concavity is bounded by raised ridges of cortical bone that trend the length of the postcanine

343   diastema. Projecting posteriorly, the post-canine diastema is moderate in length—approximately

344   62.4% of total cheek tooth series length (Table 3). Paired genial pits are positioned along the

345   posterior margin of the symphysis where rami merge to form the symphysis. A single mental

346   foramen is located along the anteroventral surface of the symphysis posteroventral of the i2

347   along both rami. Another set of foramina are evident along the postcanine diastema with the left

348   bearing three foramina and the right bearing two foramina. Rami laterally broaden in a

349   posterodorsal trend beginning ventral of p3 before being level with the base of the m3. Posterior

350   extent of the broadening appears to be evident along the labial edge of the left m3, however, due

351   to this region being heavily reconstructed this is tentative. Coracoid process originates directly

352   posterior of the m3. Angle appears to originate ventral of the m3; however, the reconstruction of

353   this portion of the rami may be skewing this observation. Submandibular fossa is lacking in

354   much of the specimen; only being evident at the posterior of the rami where it transitions into the

355   shallow pterygoid fossa along the medial surface of the angle ventral to the posterior of the m3.

356   All cheek teeth are bunodont and brachydont.

357   Anterodorsally oriented, the incisors of ETMNH 5615 exhibit a subspatulate to

358   subconical morphology with the i3 exhibiting a reduced peg-like condition (Table 4). All

359   incisors are procumbent. Wear is evident on the occlusal surface of the i1 in the development of

360   a pseudo-cylindrical wear facet comprised of an ellipsoid fossette bound by enamel. The i2 is

361   worn, with the anterior-most portion equal to the surface of the wear facet for the i1. Remaining

362 portions of the elliptical wear facet exhibit a posterolabial trend. Peg-like i3, only present on the

363 right, appears to exhibit rounding of its occlusal surface. A small diastema—approximately 7

364 mm—occurs between the i3 and anterior boundary of the canine. Canines are typical of

365 tayassuids, with a triangular outline and occlusal wear on the posterior surface.

366   Triangular in occlusal outline, the p2 of ETMNH 5615 exhibits two roots (Fig. 11).

367 Protoconid, conic in profile, is the primary cusp of the p2 and is well elevated above the talonid

368 cusp/cuspule. A weak anterior cingulum trends along the anterior surface of the protoconid.

369 Talonid cusp/cuspule is positioned directly posterolabial of the protoconid on the right p2. Left

370 p2 appears to lack this cusp due to damage and/or merger through wear. A weak lingual

371 cingulum trends from the posterolabial edge of the protoconid along the labial and posterior

372 edges of the talonid basin.

373   Trapezoidal in occlusal outline, the p3 of ETMNH 5615 exhibits four primary cusps and

374 evidence for two to three roots. Trigonid is comprised of poorly bifurcated protoconid and

375 metaconid that may merge with wear. A strong anterior cingulum is positioned along the

376 anterior base of the trigonid cusps. An accessory cuspule, or posterolabial extension of the

377 metaconid, is evident along the posterior margin of the protoconid and metaconid. Merger of

378 this feature with the metaconid through wear is present in ETMNH 5615. Talonid is comprised

379 of two rounded cusps/cuspules that are separated from the trigonid cusps (and themselves) by

380 weak valleys. A weak labial cingulum extends across the short valley between the protoconid

381 and the hypoconid. Evidence is present for a posterior cingulum but both left and right p3

382 exhibit an elongate fossette and/or damage along the posterior margin of the tooth.

383   Similar in cusp morphology to the p3, the p4 exhibits a more quadrate condition and four

384 roots. Cusps are subequal in height and conic with the trigonid cusps being elevated dorsal to the

385   talonid cusps. Weakly to moderately worn in nature, ETMNH 410 exhibits a moderate anterior

386   cingulum along the base of the trigonid. Anterior cingulum of ETMNH 5615 merges with the

387   trigonid through wear. Metaconid is merging with its posterior extension or accessory cuspule in

388   both ETMNH 410 and ETMNH 5615. Deep valleys separate the trigonid and talonid, with the

389   labial valley exhibiting a moderate cingulum between the posterior edge of the protoconid and

390   the anterior edge of the hypoconid. Entoconulid does not appear to be present in either ETMNH

391   410 or ETMNH 5615. Hypoconid exhibits anterolingual extension of its wear facet in ETMNH

392   410 toward where the entoconulid would be positioned in a molariform premolar, however, no

393   evidence of a distinct cusp is present. In ETMNH 5615 the hypoconid and entoconid wear to a

394   circular occlusal profile, with centrally positioned circular to ellipsoid fossettes. Hypoconulid

395   remains separate in both specimens being positioned along the posterolingual edge of the

396   hypoconid.

397   Despite being heavily worn in ETMNH 5615, the m1 exhibits quadrate, four rooted

398   condition. Enamel is only present along the lingual edge of the right m1 and along the entire

399   labial edge and lingual edge of the metacone of the left m1 due to the entoconid being absent.

400   Trigonid and talonid fossettes are transversally ellipsoid and completely merged. Anterior

401   margin of both the right and left m1's of ETMNH 5615 exhibit a concave depression that

402   conforms to the posterior margin of the preceding p4.

403   Heavy wear on the m2's of ETMNH 5615 is evident as the protoconid and metaconid on

404   both teeth are worn to low mounds that are merging at the median valley, now reduced to a very

405   weak furrow. Protoconid exhibits an ellipsoid fossette with an extension to the paraconule and

406   anterior cingulum. Metaconid also exhibits an ellipsoid fossette bearing an ellipsoid extension

407   into the merged posterior extension or accessory cuspule. Trigonid and talonid are still separated

408   by a moderate valley that is weak anterolingual of the entoconulid. A weak labial cingulum is

409   present between the protoconid and hypoconid. Hypoconid is merging anterolingually with the

410   entoconulid, as well as posterolingually with the hypoconulid and posterior cingulum. A circular

411   fossette dominates the center of the hypoconid with an ellipsoid extension into the site of the

412   entoconulid. Hypoconulid, despite being worn flat to the posterior cingulum, exhibits an

413   ellipsoid fossette that remains separate from the hypoconid fossette. Entoconid remains separate

414   with an ellipsoid fossette dominating the center of the cusp.

415   Cusps of the m3 of ETMNH 5615 exhibit angular wear along the anterior and posterior

416   surface with the metaconid and entoconid exhibiting less wear. A strong anterior cingulum

417   trends across the anterior of the trigonid cusps. Protoconid exhibits anterolingual merger with

418   the paraconulid and anterior cingulum. Metaconid is merged with its posterolabial extension or

419   accessory cuspule. Deep valleys separate the trigonid and talonid, while a labial cingulum trends

420   between the protoconid and hypoconid. Hypoconulid is merged anterolingually with the

421   entoconulid but remains separate from the hypoconulid. Moreover, the m3 exhibits a bulbous

422   hypoconulid complex with a single broad and robust cusp posterior to the anteroposteriorly

423   compressed hypoconulid. Left m3 exhibits merger of the hypoconulid with the heel cusp along

424   the posterolabial edge of the cuspule.

425   **Comparisons**—Specimens are attributed to *Prosthennops serus* due to the presence of a robust,

426   bunodont and brachydont dentition. At the generic level, these specimens can be differentiated

427   from *Mylohyus* based on the presence of submolariform p2's and a post-canine diastema that is

428   less than the length of the cheek tooth row. Moreover, all specimens being assigned to

429   *Prosthennops serus* exhibit a triangular p2 with a single prominent cusp anterior to the talonid;

430   further distinguishing these specimens from the lophate, subzygodont to zygodont *Protherohyus*

431   *brachydontu*s and *Platygonus pollenae.* Cranial apomorphies specific to *Prosthennops serus*

432   (e.g. distally angular zygomatic wings, zygoma originating dorsal to premolars (Wright, 1991,

433   1998)) are not evident in the GFS material due to the lack of crania.

434   Partial mandible, ETMNH 5615, is comparable to UF 212306, UF 166243, a cast of the

435   type specimen (AMNH 8511), originally described by Cope (1877), UNSM 76052, UNSM

436   76054, and UNSM 76059 (Table S1). Symphyses of these specimens exhibit a deep

437   anteroposteriorly trending semi-cylindrical spout-like concavity that opens along the posterior

438   margin of the symphysis. Moreover, each of these specimens' exhibit dentitions that are

439   bunodont and brachydont with a submolariform p2 and p3 and a molariform p4. Dentition of UF

440   212306 and UF 166243 is less worn compared to ETMNH 5615 (Fig. 11). Continuation of the

441   anterior cingulum along the anterolabial edge of the protoconid into the labial cingulum on the

442   p3 differentiates UF 212306, ETMNH 5615, UF 166243, UNSM 76052, and UNSM 76054. In

443   ETMNH 5615, UF 166243, UNSM 76052, and UNSM 76054 this cingulum terminates along the

444   anterior edge of the protoconid, with an isolated labial cingulum present within the median

445   valley between the protoconid and hypoconid. Labial cingulum trends posteriorly along the

446   labial edge of the hypoconid in UF 166243. A labial cingulum is also observed in the p4 with

447   ETMNH 5615, UF 212306, UNSM 76052, UNSM 76054, and UNSM 76059 exhibiting a labial

448   cingulum that is restricted within the median valley. Alternatively, UF 166243 exhibits an

449   extension of the cingulum along the labial to posterior margin of the hypoconid of the p4. None

450   of the observed specimens adequately represent the cusps of the m1 due to wear or loss through

451   damage. Remaining molars exhibit a similar morphology, with ETMNH 5615 exhibiting more

452   labiolingually broad and robust anterior and posterior cingula of the m2 and m3 than UF 212306,

453   UF/TRO 413, UF 166243, UNSM 76052, UNSM 76054, or UNSM 76059. Both UF 220251

454 and UF/TRO 413 exhibit m3's that are comparable to ETMNH 5615, UF 212306, UNSM 76052,

455 UNSM 76054, and UNSM 76059 due to the relative morphology of the cusps and the

456 hypoconulid complex being dominated by two to three poorly bifurcated accessory cusps that

457 may merge together through wear into a single prominent cusp. Overall, ETMNH 5615, UF

458 212306, UF220251, and UF/TRO 413 exhibit similar dental and mandibular characteristics to the

459 cast of the type specimen—UF 166243—and those described in Hesse (1935), Colbert (1938),

460 and Schultz and Martin (1975); however, dental dimensions vary within the sample (Fig. 11).

461 Specimens from the GFS and Tyner Farm Locality are proportionally larger than the material

462 described by Hesse (1935), Colbert (1938), and Schultz and Martin (1975), indicating greater

463 interspecific variation than previously recognized.

464 **DISCUSSION**

465   Previously only known from the Palmetto Fauna of Florida (Wright & Webb, 1984; Wright,

466 1991, 1998) within the Fort Green Mine, Palmetto Mine, Payne Creek, Saddle Creek Mine, and

467 South Pierce quarries, *M. elmorei* exhibits a northward expansion into the Appalachian region

468 with the inclusion of GFS material (Fig 1). Although this discovery expands the range of *M.*

469 *elmorei*, it does not negate the assertion by Webb et al. (2008) that the species is endemic to the

470 southeastern North America. *Mylohyus*, as a genus, is widespread throughout parts of North

471 America (Wright, 1998). *Mylohyus fossilis* in particular is prevalent through the Blancan to

472 Rancholabrean of the central and southeastern regions of North America (Kinsey, 1974; Kurten

473 & Anderson, 1980; Wright, 1991, 1998). Alternatively, another Hemphillian species within the

474 genus, *M. longirostris*, is reported from the John Day region based on a single rami and

475 fragmentary cranial material (Thorpe, 1924; Wright, 1991, 1998). Wright (1998) attributes

476 material collected from the Hemphillian Mixon's Bone Bed local fauna of Florida as being

477   affiliated to *M. longirostris*; however, only the locality is designated. No specimen data is

478   reported to verify this record. In sum, the geographic distribution of these species illustrates the

479   potential for a larger distribution for *M. elmorei*, however, the rarity of the species within given

480   localities can make further range expansions difficult to determine.

481   Confirmation of *Prosthennops serus* at the GFS expands the known range of the taxon

482   eastward and northward into the Appalachian Mountain region, making GFS the second eastern-

483   most locality from which *Prosthennops serus* is recognized (Fig. 1). Following Wright (1998),

484   *Prosthennops serus—senso stricto—*is known from the early Clarendonian of Kansas (Cope,

485   1877; Wright, 1998), earliest Hemphillian of Oregon (Colbert, 1938), earliest to late early

486   Hemphillian of Nebraska (Hesse, 1935; Schultz & Martin, 1975), earliest Hemphillian to

487   Blancan of an unnamed unit within Hidalgo, Mexico (Wright, 1998), late early Hemphillian of

488   Alabama (Hulbert & Whitmore, 2006), and early Hemphillian Tyner Farm locality of Florida

489   (Hulbert et al., 2009a). Material from the late to latest Hemphillian of the Coffee Ranch Fauna

490   of Texas— approximately 6.6 Ma (Passey et al., 2002)—and Ocote Fauna of Mexico are also

491   referred by Wright (1998), however, no catalog numbers are listed resulting in ambiguity

492   regarding whether this refers to new or reassigned material.   Other localities listed by Wright

493   (1998) as bearing material comparable to *Prosthennops serus* are located within the earliest

494   Hemphillian of the Deer Lodge Basin of Montana, late early Hemphillian Higgins Local Fauna

495   of Texas, and late early Hemphillian of the Wray Fauna of Colorado. Webb and Perrigo (1984)

496   also refer a well-worn m3 as being comparable to the species from the Gracias Fm. of Honduras,

497   however, the worn nature of the tooth and predominant use of anteroposterior and transverse

498   measurements make this identification suspect.

499   Overall, the presence of *M. elmorei* and *Prosthennops serus* within the fauna of the GFS

500   provides further evidence for a forested environment. Additionally, their presence draws further

501   parallels to the Palmetto Fauna. *Mylohyus elmorei* and *Protherohyus brachydontus* within the

502   Palmetto Fauna are referred to by Webb et al. (2008) as browse-dominated mixed-feeders.

503   DeSantis and Wallace (2008) report that two of the GFS tayassuid specimens exhibit a C 3

504   dominated dietary profile. Despite the specimens being attributed to *M. elmorei* and

505   *Prosthennops serus* not being recovered until after DeSantis and Wallace (2008), a similar

506   browsing diet is suggested for the GFS *M. elmorei* and *Prosthennops serus* material based on

507   morphology. Specifically, the presence of a bunodont and brachydont dentition is cited by

508   Hulbert (2001) as an indicator for *M. fossilis* being a forest species that subsisted on fruit, nuts,

509   and succulents. Additional evidence for this dietary preference in fossil peccaries, including *M.*

510   *elmorei*, has been reported using stable carbon isotope and dental microwear texture analyses

511   (Yann and DeSantis, 2014; Bradham et al., 2018). Similar parallels are drawn by Woodburne

512   (1968), Kiltie (1981), Sowls (1997) and Wright (1998) based on observations on the populations

513   of modern woodland populations of *Pecari* (=*Dicotyles*) *tajacu* and *Tayassu pecari*.

514   Additionally, potential dental pathologies (e.g. caries such as those described by Andrews

515   (1973), Coyler (1990), Figueirido et al. (2017), and Wang et al. (2017)) on the m1's of ETMNH

516   8046 further suggest a frugivorous or sugar-rich diet that would fit in with the current

517   interpretation of the site being an oak-hickory forest.

518   Recent assessment of the mammalian fauna suggests an age of 4.9 to 4.5 Ma for the GFS

519   (Samuels, Bredehoeft & Wallace, 2018). This suggestion brings the maximum age of the GFS to

520   be in line with that of the Palmetto Fauna of Florida, which is interpreted to be 5.0-4.5 Ma

521   (Tedford et al., 2004; Webb et al., 2008). Presence of *M. elmorei* could be used to reinforce the

522   upper age limit of GFS, however, there is a possibility that the GFS represents an earlier or later

523   record for *M. elmorei*. Moreover, the presence of *Prosthennops serus* at the GFS cannot be

524   utilized to constrain the age due to the species being known from the latest Clarendonian to

525   earliest Blancan (Wright, 1998). Further verification of material from other sites and radiometric

526   analyses, where permissible, are needed to utilize any of the GFS tayassuids for further

527   constraining the site's biochronology.

528   **CONCLUSIONS**

529   Within the GFS tayassuid material a total of two individuals attributed to *M. elmorei* and

530   *Prosthennops serus*, respectively, are recognized through systematic analyses. Accordingly, the

531   known distribution of *M. elmorei* and *Prosthennops serus* is expanded north into the

532   Appalachian region; the first reported instance of *M. elmorei* outside the Palmetto Fauna of

533   Florida. Moreover, the presence of *M. elmorei* emphasizes further parallels between the

534   Palmetto Fauna and the GFS reinforcing the paleoenvironmental interpretation of the latter and

535   suggesting a greater connectivity between the faunas than previously thought.   Indeterminant

536   tayassuid material that cannot be directly assigned to either species is evident within the GFS

537   fauna, however, the limited and fragmentary nature of the remaining tayassuid material prevents

538   the designation of another species at this time. Future work focused on this material, in

539   particular the postcranial material, is necessary to further discern the ecology and morphological

540 variation of these species both within the GFS and late Hemphillian to early Blancan of North

541 America.

542 **ACKNOWLEDGMENTS**

543   We thank Jim Mead for comments and suggestions on an earlier version of this

544 manuscript. Moreover, further thanks are due to Sandra Swift for her aid and overall support

545 throughout the project. Additional thanks to Shawn Haugrud, Brian Compton, April Nye, and

546 Anthony Woodward for their assistance in ETSU collections. We thank Dr. Richard Hulbert for

547 providing access to the University of Florida (UF) collections and providing references and

548 feedback related to the collection. Recognition for the photography goes to Sean Moran.

549 Express thanks are also due to Dr. James Farlow and Ronald Richards for providing access and

550 consultation regarding the tayassuid material associated with the Pipe Creek paleosinkhole. We

551 thank Dr. Hugh "Greg" McDonald for his assistance in clarifying morphological nomenclature.

552 Lastly, we thank reviewers for their helpful comments and edits to this manuscript.

553 **REFERENCES**

554 Andrews AH. 1973. Dental caries in an experimental domestic pig. *The Veterinary record*

555   93:257–258.

556 Bradham JL., DeSantis LRG., Jorge MLSP., Keuroghlian A. 2018. Dietary variability of extinct

557   tayassuids and modern white-lipped peccaries *(Tayassu pecari)* as inferred from dental

558   microwear and stable isotope analysis. *Palaeogeography, Palaeoclimatology,*

559   *Palaeoecology* 499:93–101.

560 Bourque JR., Schubert BW. 2015. Fossil musk turtles (Kinosternidae, Sternotherus) from the late

561   Miocene–early Pliocene (Hemphillian) of Tennessee and Florida. *Journal of Vertebrate*

562   *Paleontology* 35:1–19. DOI: 10.1080/02724634.2014.885441.

563   Colbert EH. 1938. Pliocene peccaries from the Pacific Coast region of North America. *Carnegie*

564   *Institute of Washington Publication* 487:241–269.

565   Cope ED. 1877. Descriptions of new Vertebrata from the upper Tertiary formations of the West.

566   *Proceedings of the American Philosophical Society* 17:219–231.

567   Cope ED. 1889. The Artiodactyla (Continued). *The American Naturalist* 23:111–136.

568   Coyler JF. 1990. *Colyer's variations and diseases of the teeth of animals, revised edition*.

569   Cambridge: Cambridge University Press. DOI: 10.1017/CBO9780511565298.

570   DeSantis LRG., Wallace SC. 2008. Neogene forests from the Appalachians of Tennessee, USA:

571   Geochemical evidence from fossil mammal teeth. *Palaeogeography, Palaeoclimatology,*

572   *Palaeoecology* 266:59–68. DOI: 10.1016/j.palaeo.2008.03.032.

573   Farlow JO., Sunderman JA., Havens JJ., Swinehart AL., Holman JA., Richards RL., Miller NG.,

574   Martin RA., Hunt Jr RM., Storrs GW., Curry BB., Fluegeman RH., Dawson MR., Flint

575   MET. 2001. The Pipe Creek Sinkhole Biota, a diverse Late Tertiary continental fossil

576   assemblage from Grant County, Indiana. *American Midland Naturalist* 145:367–378.

577   Figueirido B., Pérez-Ramos A., Schubert BW., Serrano F., Farrell AB., Pastor FJ., Neves AA.,

578   Romero A. 2017. Dental caries in the fossil record: a window to the evolution of dietary

579   plasticity in an extinct bear. *Scientific Reports* 7:1–7. DOI: 10.1038/s41598-017-18116-0.

580   Gidley JW. 1904. New or little known mammals from the Miocene of South Dakota: American

581   Museum Expedition of 1903. (By WD Matthew and JW Gidley, Part. III, Dicotylidae by

582   JW Gidley). *Bulletin of the American Museum of Natural History* 20:241–268.

583 Hesse CJ. 1935. A vertebrate fauna from the type localiity of the Ogallala Formation. *University*
584   *of Kansas Science Bulletin* 32:79–118.

585 Hulbert RC. 2001. *The fossil vertebrates of Florida*. Gainesville: University Press of Florida.

586 Hulbert RC., Morgan GS., Kerner A. 2009a. Collared Peccary (Mammalia, Artiodactyla,
587   Tayassuidae, Pecari) from the Late Pleistocene of Florida. *Papers on Geology, Vertebrate*
588   *Paleontology, and Biostratigraphy in Honor of Michael O. Woodburne. Museum of*
589   *Northern Arizona Bulletin 65, Flagstaff, Arizona.* 65:543–556.

590 Hulbert RC., Wallace SC., Klippel WE., Parmalee PW. 2009b. Cranial morphology and
591   systematics of an extraordinary sample of the late Neogene dwarf tapir, Tapirus polkensis
592   (Olsen). *Journal of Paleontology* 83:238–262.

593 Hulbert RC., Whitmore FC. 2006. Late Miocene mammals from the Mauvilla Local Fauna,
594   Alabama. *Bulletin of the Florida State Museum* 46:1–28.

595 Kiltie RA. 1981. Stomach contents of rain forest peccaries (Tayassu tajacu and T. pecari).
596   *Biotropica* 13:234–236.

597 Kinsey PE. 1974. A New Species of *Mylohyus* Peccary from the Florida Early Pleistocene. In:
598   Webb SD ed. *Pleistocene Mammals of Florida*. University Presses of Florida, 158–169.

599 Kurten B., Anderson E. 1980. *Pleistocene mammals of North America*. New York: Columbia
600   University Press.

601 Linnaeus C. 1758. *Systema naturae per regna tria naturae: secundum classes, ordines, genera,*
602   *species, cum characteribus, differentiis, synonymis, locis*. Stockholm: Tomus I. L. Salvii.

603 Liu YSC., Jacques FMB. 2010. *Sinomenium macrocarpum* sp. nov. (Menispermaceae) from the

604   Miocene--Pliocene transition of Gray, northeast Tennessee, USA. *Review of Palaeobotany*

605   *and Palynology* 159:112–122.

606   Mcdonald HG., De Muizon C. 2002. The cranial anatomy of Thalassocnus (Xenarthra,

607   Mammalia), a derived nothrothere from the Neogene of the Pisco Formation (Peru). *Journal*

608   *of Vertebrate Paleontology* 22:349–365. DOI: 10.1671/0272-

609   4634(2002)022[0349:TCAOTX]2.0.CO;2.

610   De Muizon C., Mcdonald HG., Salas R., Urbina M. 2003. A new early species of the aquatic

611   sloth Thalassocnus (Mammalia, Xenarthra) from the Late Miocene of Peru. *Journal of*

612   *Vertebrate Paleontology* 23:886–894. DOI: 10.1671/2361-13.

613   Ochoa D., Whitelaw M., Liu YSC., Zavada M. 2012. Palynology of Neogene sediments at the

614   Gray Fossil Site, Tennessee, USA: Floristic implications. *Review of Palaeobotany and*

615   *Palynology* 184:36–48. DOI: 10.1016/j.revpalbo.2012.03.006.

616   Owen R. 1848. Description of teeth and portions of jaws of two extinct anthracotherioid

617   quadrupeds (Hyopotamus vectianus and Hyop. bovinus) discovered by the Marchioness of

618   Hastings in the Eocene deposits on the NW coast of the Isle of Wight: with an attempt to

619   develop. *Quarterly Journal of the Geological Society of London* 4:104–141.

620   Palmer TS. 1897. Notes on the nomenclature of four genera of tropical American mammals.

621   *Proceedings of the Biological Society of Washington* 11:173–174.

622   Parisi Dutra R., de Melo Casali D., Missagia RV., Gasparini GM., Perini FA., Cozzuol MA.

623   2016. Phylogenetic systematics of peccaries (Tayassuidae: Artiodactyla) and a classification

624   of South American tayassuids. *Journal of Mammalian Evolution* 24:345–358.

625   Parmalee PW., Klippel WE., Meylan PA., Holman JA. 2002. A Late Miocene-Early Pliocene

626   population of *Trachemys* (Testudines: Emydidae) from east Tennessee. *Annals of Carnegie*

627   *Museum* 71:233–239.

628   Passey BH., Cerling TE., Perkins ME., Voorhies MR., Harris JM., Tucker ST. 2002.

629   Environmental change in the Great Plains: an isotopic record from fossil horses. *The*

630   *Journal of Geology* 110:123–140.

631   Prothero DR., Sheets HA. 2013. Peccaries (Mammalia, Artiodactyla, Tayassuidae) from the

632   Miocene-Pliocene Pipe Creek Sinkhole Local Fauna, Indiana. *Kirtlandia* 58:54–60.

633   Samuels JX., Bredehoeft KE., Wallace SC. 2018. A new species of *Gulo* from the Early Pliocene

634   Gray Fossil Site (Eastern United States); rethinking the evolution of wolverines. *PeerJ*

635   6:e4648. DOI: 10.7717/peerj.4648.

636   Schultz CB., Martin LD. 1975. A new Kimballian peccary from Nebraska. *Bulletin of the*

637   *University of Nebraska State Museum* 10:35–46.

638   Short RA. 2013. A new species of *Teleoceras* from the Late Miocene Gray Fossil Site, with

639   comparisons to other North American Hemphillian species. *Electronic Theses and*

640   *Dissertations*. Paper 1143. https://dc.etsu.edu/etd/1143.

641   Shunk AJ., Driese SG., Clark GM. 2006. Latest Miocene to earliest Pliocene sedimentation and

642   climate record derived from paleosinkhole fill deposits, Gray Fossil Site, northeastern

643   Tennessee, U.S.A. *Palaeogeography, Palaeoclimatology, Palaeoecology* 231:265–278.

644   DOI: 10.1016/j.palaeo.2005.08.001.

645   Shunk AJ., Driese SG., Farlow JO., Zavada MS., Zobaa MK. 2009. Late Neogene paleoclimate

646   and paleoenvironment reconstructions from the Pipe Creek Sinkhole, Indiana, USA.

647   *Palaeogeography, Palaeoclimatology, Palaeoecology* 274:173–184. DOI:

648   10.1016/j.palaeo.2009.01.008.

649   Sisson S., Grossman JD. 1975. *The anatomy of the domestic animals*. Philadelphia: W.B.

650   Saunders Co.

651   Sowls LK. 1997. *Javelinas and other peccaries: their biology, management, and use*. College

652   Station: Texas A&M University Press.

653   Tedford RH., Albright III LB., Barnosky AD., Ferrusquia-Villafranca I., Hunt Jr RM., Storer JE.,

654   Swisher III CC., Voorhies MR., Webb SD., Whistler DP., others. 2004. Mammalian

655   biochronology of the Arikareean through Hemphillian interval (late Oligocene through early

656   Pliocene epochs). In: *Late Cretaceous and Cenozoic mammals of North America:*

657   *biostratigraphy and geochronology*. New York: Columbia University Press, 169–231.

658   Thorpe MR. 1924. A new species of extinct peccary from Oregon. *American Journal of Science*

659   41:393–397. DOI: 10.1017/S1355617712001555.

660   Von den Driesch A. 1976. *A guide to the measurement of animal bones from archaeological*

661   *sites*. Cambridge: Peabody Museum Bulletins, Harvard University.

662   Wallace SC., Wang X. 2004. Two new carnivores from an unusual late Tertiary forest biota in

663   eastern North America. *Nature* 431:556–559.

664   Wang X., Rybczynski N., Harington CR., White SC., Tedford RH. 2017. A basal ursine bear

665   (Protarctos abstrusus) from the Pliocene High Arctic reveals Eurasian affinities and a diet

666   rich in fermentable sugars. *Scientific Reports* 7:17722. DOI: 10.1038/s41598-017-17657-8.

667 Webb SD., Hulbert Jr. RC., Morgan GS., Evans HF. 2008. Terrestrial mammals of the Palmetto

668   Fauna (early Pliocene, latest Hemphillian) from the central Florida phosphate district.

669   *Natural History Museum Los Angeles County Science Series* 41:293–312.

670 Webb SD., Perrigo SC. 1984. Late Cenozoic Vertebrates from Honduras and El Salvador.

671   *Journal of Vertebrate Paleontology* 4:237–254.

672 White TE. 1942. Additions to the fauna of the Florida phosphates. In: *Proceedings of the New*

673   *England Zoology Club*. 87–91.

674 Whitelaw JL., Mickus K., Whitelaw MJ., Nave J. 2008. High-resolution gravity study of the

675   Gray Fossil Site. *Geophysics* 73:25–32.

676 Woodburne MO. 1968. The cranial myology and osteology of *Dicotyles tajacu*, the collared

677   peccary, and its bearing on classification. *Memoirs of the Southern California Academy of*

678   *Sciences* 7:1–48.

679 Wright DB. 1989. Phylogenetic relationships of *Catagonus wageni*: sister taxa from the Tertiary

680   of North America. *Advances in Neotropical Mammalogy*:281–308. DOI:

681   10.1017/S1355617712001555.

682 Wright DB. 1991. Cranial morphology, systematics, and evolution of neogene Tayassuidae

683   (Mammalia). D. Phil. Thesis, University of Massachusetts.

684 Wright DB. 1998. Tayassuidae. *Evolution of tertiary mammals of North America* 1:389–401.

685 Wright DB., Webb SD. 1984. Primitive *Mylohyus* (Artiodactyla: Tayassuidae) from the late

686   Hemphillian Bone Valley of Florida. *Journal of Vertebrate Paleontology* 3:152–159.

687 Yann LT., DeSantis LRG. 2014. Effects of Pleistocene climates on local environments and

688   dietary behavior of mammals in Florida. *Palaeogeography, Palaeoclimatology,* and

689   *Palaeoecology* 414:370–381.

Measurements (mm) of the upper dentition and cranium of *Mylohyus elmorei*.

Approximate measurements are marked by (*).

	N	X̄	Range		σ²	σ	ETMNH 8046 Left	Right	Average	UF 12265 Left	Right	Average	UF 203540	UF/TRO 440
Length P2-M3	2	96.45	94.91	- 98.00	2.38	1.54	97.68	98.31	98.00	94.91				
Length P2-P4	2	37.40	37.35	- 37.46	0.00	0.06	36.78	37.91	37.35	37.46				
Length M1-M3	2	59.20	57.20	- 61.20	4.01	2.00	61.27	61.13	61.20	57.20				
Post Canine Diastema	2	101.59	95.68	- 107.51	34.95	5.91	107.51			95.68*				
% Length of PCD/ Length P2-M3	2	105	101	- 110	0.00	5	110			101				
Height of Canine Buttress	1	51.21					51.21							
Canine APA	1	22.52					22.52							
Transverse	1	15.60					15.60							
P2 APO	2	10.34	10.31	- 10.36	0.00	0.02	10.37	10.25	10.31	10.36				
AT	2	9.50	9.32	- 9.69	0.03	0.19	9.69	9.69	9.69	9.32				
PT	2	9.47	9.32	- 9.63	0.02	0.15	9.67	9.58	9.63	9.32				
P3 APO	2	12.44	12.36	- 12.51	0.01	0.08	12.49	12.54	12.51	12.36				
AT	2	11.39	11.36	- 11.42	0.00	0.03	11.39	11.45	11.42	11.36				
PT	2	12.24	12.20	- 12.28	0.00	0.04	12.09	12.31	12.20	12.28				
P4 APO	2	14.31	14.25	- 14.38	0.00	0.07	14.28	14.48	14.38	14.25				
AT	2	12.69	12.22	- 13.17	0.23	0.48	12.01	12.42	12.22	13.17				
PT	2	14.26	13.98	- 14.54	0.08	0.28	13.68	14.29	13.98	14.54				
M1 APO	2	17.63	17.09	- 18.17	0.29	0.54	18.33	18.00	18.17	17.09				
AT	2	16.16	16.11	- 16.20	0.00	0.05	16.09	16.13	16.11	16.20				
PT	2	16.38	16.33	- 16.43	0.00	0.05	16.44	16.41	16.43	16.33				
M2 APO	2	19.33	19.07	- 19.58	0.07	0.26	19.62	19.54	19.58	19.16	18.98	19.07		
AT	2	17.57	17.30	- 17.84	0.07	0.27	17.88	17.81	17.84	17.23	17.38	17.30		
PT	2	16.84	16.14	- 17.55	0.50	0.71	17.66	17.44	17.55	16.02	16.29	16.14		
M3 APO	4	22.57	21.29	- 23.36	0.69	0.83	23.57	23.14	23.36	21.33	21.27	21.29	22.36	23.26
AT	4	17.18	15.59	- 18.79	1.35	1.16	16.91	16.66	16.78	15.53	15.65	15.59	17.55	18.79
PT	4	13.76	12.34	- 14.91	1.33	1.16	14.97	14.81	14.89	12.35	12.34	12.34	12.91	14.91
HT	2	9.19	8.98	- 9.40	0.04	0.21	9.29	9.51	9.40	8.86	9.09	8.98		

Measurements (mm) of the lower dentition and mandible of *Mylohyus elmorei*.

Approximate measurements are marked by (*) whereas incomplete measurements, due to the posterior portion of enamel being absent, are marked by (+).

		N	X̄	Range	σ^2	Σ	Left	Right	Average	ETMNH 17219	ETMNH 19281	UF 57280 Cast of holotype	UR/TRO 412	UF 294749
Length p2-m3		1	100.81					100.81	100.81					
Length p2-p4		1	39.94					39.94	39.94					
Length m1-m3		2	60.29	59.84-60.95	0.21	0.46	60.95	60.55	60.75				59.84	
Depth of rami at m1		1	43.98					42.69	43.98					
Depth of rami at m3		1	43.00					42.71	43.00					
p2	APO	3	11.98	11.17-12.78	0.43	0.66		11.17	11.17			11.99		
	AT	3	7.87	6.63-9.12	1.04	1.02		6.63	6.63			7.87		
	PT	3	8.37	7.88-8.72	0.13	0.36		7.88	7.88			8.52		
p3	APO	2	13.62	13.55-13.69	0.00	0.07	13.47	13.64	13.55	13.5+			13.69	
	AT	3	10.92	10.02-12.70	1.59	1.26	10.09	9.99	10.04	10.26		12.70	10.02	
	PT	3	11.22	10.69-11.53	0.14	0.38	10.62	10.75	10.69	10.62		11.53*	11.44	
p4	APO	5	14.67	12.74-16.83	1.69	1.30	14.75	14.70	14.73			14.62	14.44	12.74
	AT	5	12.63	11.98-14.19	0.63	0.79	11.97	11.99	11.98			14.19	12.47	12.29
	PT	5	13.63	12.53-16.22	1.74	1.32	12.94	13.07	13.01			16.22	13.36	13.05
m1	APO	3	16.49	16.20-16.84	0.07	0.27	16.35	16.52	16.44			16.84	16.20	
	AT	3	13.43	13.12-13.72	0.06	0.24	13.62	13.81	13.72			13.12	13.45	
	PT	3	14.73	13.86-16.41	1.41	1.19	13.88	13.84	13.86			16.41	13.92	
m2	APO	4	19.52	17.74-21.88	2.55	1.60	18.48	18.38	18.43		20.03	21.88	17.74	
	AT	4	15.40	14.30-18.00	2.28	1.51	14.22	14.37	14.30		14.69	18.00	14.60	
	PT	4	15.86	14.56-19.00	3.37	1.83	14.58	14.53	14.56		15.28	19.00	14.61	
m3	APO	3	26.22	25.36-27.75	1.18	1.09	25.45	25.26	25.36			27.75	25.55	
	AT	3	15.64	13.37-18.97	5.80	2.41	13.32	13.42	13.37			18.97	14.57	
	PT	3	14.75	13.02-18.10	5.62	2.37	13.12	13.13	13.13			18.10	13.02	
	HT	3	11.24	9.94-13.78	3.22	1.79	10.04	9.97	10.00			13.78	9.94	

Measurements (mm) of the lower dentition and mandible of *Prosthennops serus*.

Approximate measurements are marked by (*). Additional measurement data is taken from (T) Schultz and Martin (1975), (H) Hesse (1935), and (C) Colbert (1938).

	N	$\bar{X}$	Range		σ^2	σ	ETMNH 5615			UF 166243 Type Cast (AMNH8511)	UF 212306	UNSM 76052[T]	UNSM 76504[T]	KUMP 3755[H]	C.I.T 610[C]
							Left	Right	Average						
Length p2-m3	5	97.71	91.60	-	103.06	22.86	4.78	101.95	104.16	103.06		102.41*	91.60	92.70	98.80	
Length p2-p4	7	38.23	36.00	-	40.27	1.95	1.40	37.39	39.15	38.27	38.41	40.27	36.00	36.50	39.20	39.00
Length m1-m3	5	59.42	53.50	-	15.98	4.00	4.16	64.22	65.18	64.70		62.50	53.50	56.70	59.70	
Postcanine Diastema	6	54.87	49.90	-	62.40	28.33	5.32	61.17	63.62	62.40		62.04*	51.50	49.90	53.40	50.00
% Length of PCD/Length p2-m3	1	0.605	0.60	-	0.61	0.00	0.00			0.61		0.60				
Precanine Diastema	3	6.75	6.26	-	7.50	0.29	0.54	6.01	6.51	6.26			7.50	6.50		
Length Mandibular symphysis	3	86.14	82.00	-	90.28	17.13	4.14		92.33			90.28				82.00
Distance between p2 and symphysis	1								10.66							
Depth of rami at m3	1	39.22										39.22				
Depth of rami at m1	3	45.79	42.27	-	50.02	10.25	3.20	48.72	51.32	50.02		42.27	45.10			
Width of rami at m3	1	24.91										24.91				

Measurements (mm) of the lower dentition and mandible of *Prosthennops serus*.

Approximate measurements are marked by (*). Additional measurement data is taken from (T) Schultz and Martin (1975), (H) Hesse (1935), and (C) Colbert (1938).

		N	X̄	Range			σ^2	σ	Left	Right	Average	ETMNH 410	UF 166243 Type Cast (AMNH8511)
									ETMNH 5615				
i1	APO	1	8.40				0.00	0.00	8.37	8.43	8.40		
	AT	2	5.90	4.50	-	7.30	1.96	1.40	7.06	7.55	7.30		
	PT	0											
i2	APO	3	9.94	5.41	-	12.70	10.42	3.23		5.41	5.41		
	AT	4	6.59	5.00	-	8.56	1.80	1.34	8.41	8.71	8.56		
	PT	0											
i3	APO	2	5.11	4.70	-	5.51	0.16	0.40		5.51	5.51		
	AT	3	3.19	2.50	-	4.47	0.82	0.90		4.47	4.47		
	PT	0											
Canine	APA	5	16.33	13.74	-	18.40	3.11	1.76	13.7		13.74		
	Transvers	4	13.21	12.24	-	14.60	0.86	0.93	11.9	12.57	12.24		
p2	APO	7	10.79	9.92	-	11.25	0.20	0.45	9.79	10.06	9.92		10.93
	AT	6	6.93	6.39	-	7.60	0.17	0.41	6.31	6.46	6.39		6.54
	PT	3	7.25	7.16	-	7.33	0.01	0.07	7.19	7.37	7.28		7.16
p3	APO	7	12.49	11.80	-	13.00	0.12	0.35	12.7	12.53	12.65		12.48
	AT	6	9.34	9.00	-	9.70	0.06	0.25	9.01	9.26	9.14		9.22
	PT	3	9.41	9.31	-	9.61	0.02	0.14	9.48	9.73	9.61		9.33
p4	APO	8	15.08	13.20	-	17.36	1.36	1.16	15.7	16.14	15.94	17.36	15.00
	AT	7	11.97	11.07	-	12.64	0.21	0.46	11.5	12.00	11.78	11.07	11.86
	PT	4	13.10	12.40	-	13.85	0.30	0.55	13.1	13.55	13.36	12.78	12.40
m1	APO	7	14.83	13.70	-	15.98	0.56	0.75	14.9	14.98	14.96		15.38
	AT	6	12.61	12.00	-	13.20	0.19	0.43	12.9	12.78	12.87		12.10
	PT	3	13.04	12.19	-	13.96	0.53	0.73		12.97	12.97		12.19
m2	APO	8	18.82	16.80	-	20.77	1.35	1.16	20.5	21.02	20.77		19.71
	AT	7	14.98	14.00	-	16.00	0.46	0.68	16.0	15.99	16.00		15.51
	PT	4	15.84	15.42	-	16.40	0.12	0.35	16.2	16.54	16.40		15.42
m3	APO	7	27.61	24.50	-	32.26	5.92	2.43	29.4	29.77	29.63		
	AT	7	16.14	14.90	-	18.52	1.32	1.15	16.6	16.73	16.67		15.51
	PT	5	16.09	14.86	-	17.60	0.95	0.97	16.4	16.77	16.58		14.86
	HT	4	12.61	12.29	-	13.14	0.10	0.32	12.5	12.53	12.54		

		UF 220251	UF 212306	UF/TRO 413	UNSM 76052[T]	UNSM 76504[T]	KUMP 3755[H]	C.I.T 610[C]
i1	APO							
	AT							4.50
	PT							
i2	APO				12.70	11.70		
	AT				7.00	5.80		5.00
	PT							
i3	APO					4.70		
	AT					2.60		2.50
	PT							
Canine	APA				18.40*	16.50	18.00	15.00
	Transverse				14.60*	12.50		13.50
p2	APO		11.25		11.00	10.30	11.10	11.00
	AT		7.26		7.60	6.80		7.00
	PT		7.33					
p3	APO		13.00		11.80	12.70	12.30	12.50
	AT		9.39		9.70	9.60		9.00
	PT		9.31					
p4	APO		15.62*		13.20	14.70	14.30	14.50
	AT		12.64		12.40	12.00		12.00
	PT		13.85					
m1	APO		15.98*		15.30	13.70	14.00	14.50
	AT		12.89		13.20	12.60*		12.00
	PT		13.96					
m2	APO		19.23	18.73	16.80	18.60	19.20	17.50
	AT		14.84	15.58	14.40	14.50		14.00
	PT		15.74	15.80				
m3	APO	32.26	28.14	26.57	24.50	25.80	26.40	
	AT	18.52	16.32	16.03	14.90	15.00		
	PT	17.60	16.17	15.25				
	HT	13.14	12.48	12.29				

Figure 1

Eastern to southeast United States (US) showing locations of the Hemphillian sites bearing peccary material (A).

The Gray Fossil Site (top right) is located in north-central Washington County (B), TN at 36.5°N and 82.5°W. *Mylohyus elmorei* is previously only known from various localities within the Phosphate Mines (grey) of the Palmetto Fauna (bottom right) (C) (Wright and Webb, 1984; Wright, 1991, 1998). Wright (1998) reports material with affinity to *Mylohyus longirostris* from the Mixon's Bone Bed local fauna of northern Florida; however, no specimens are directly listed to verify this claim. *Prosthennops serus* is identified within the Mauville Fauna of southern Alabama (Hulbert and Whitemore, 2006) and the Tyner Farm locality of northern Florida (Hulbert et al. 2009a). *Protherohyus brachydontus* (=*Catagonus brachydontus*), despite being widespread in the western US and Mexico, is currently only recognized in the Palmetto Fauna (Wright 1989, 1991, 1998) and the Pipe Creek paleosinkhole of Indiana (Prothero and Sheets, 2013) in the eastern US.

(A)

(B)

(C)

Polk

Hillsborough

Manatee

Hardee

Legend

★ Gray Fossil Site

◇ *Mylohyus elmorei*

■ *Mylohyus longirostrus*

◆ *Protherohyus brachydontus*

✕ *Prosthennops serus*

N

0   325   650   1,300
Kilometers

N

0   15   30   60
Kilometers

N

0   5   10
Kilometers
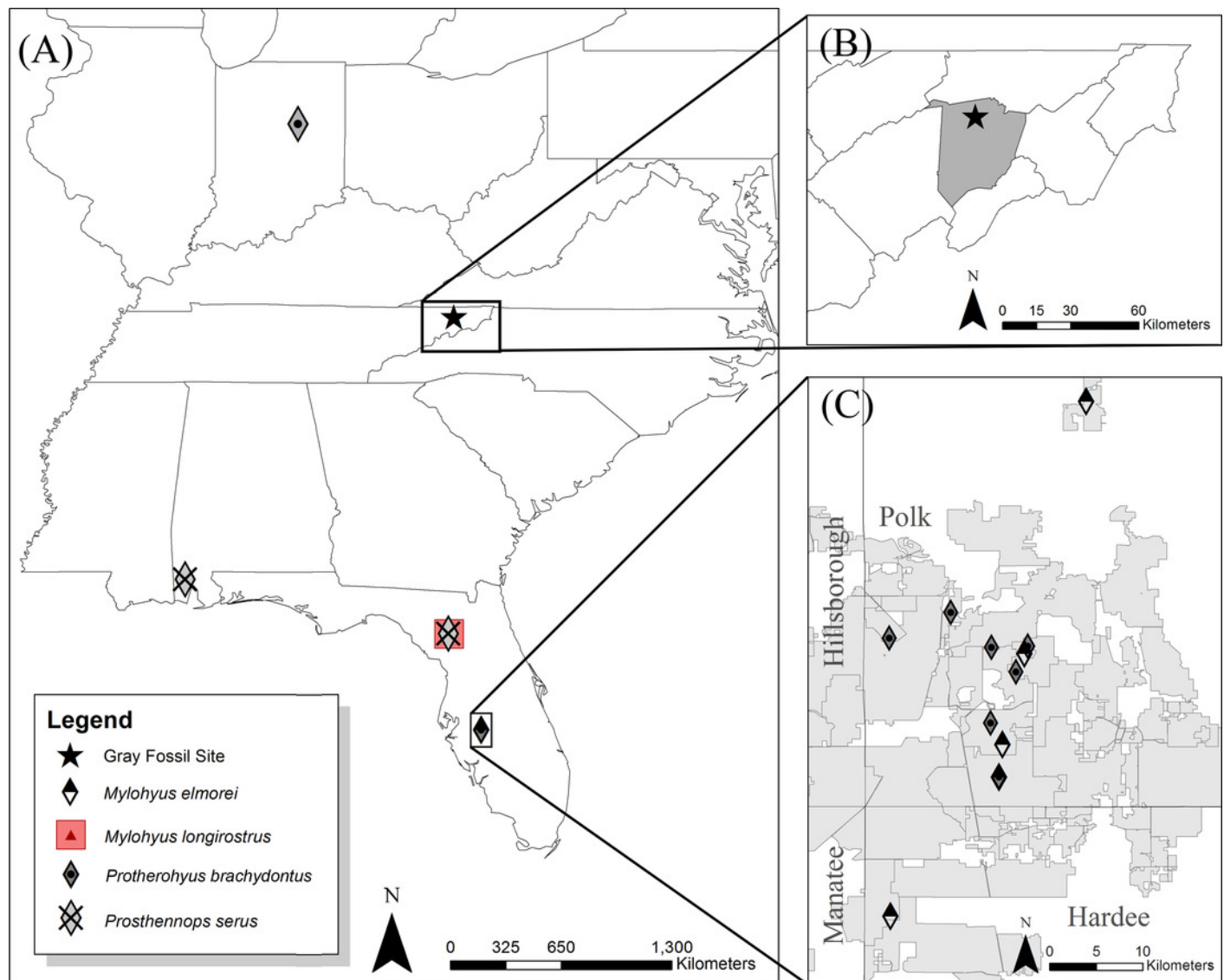
Figure 2

Measurements for tayassuid cranial (A and B) and mandibular (C and D) material (ETVP 17584, an adult *Pecari tajacu*).

Measurements are modified from Von den Driesh (1976) with the abbreviation PCD representing postcanine diastema.

(A)

Height of
canine buttress

PCD

(B)

PCD

Length P2-P4   Length M1-M3

Length P2-M3

(C)

Length m1-m3

Length of mandibular
symphysis (across
ventral surface)

Length p2-p4

PCD

Precanine
diastema

Length p2-m3

(D)

Precanine
diastema

PCD

Depth
at rami
at m3

Depth
at rami
at m1

Length of
mandibular
symphysis

Figure 3

Dental measurements for both upper and lower dentition (A) follow Wright (1984, 1991) with the addition the transverse measurement across the hypoconule/hypoconulid complex.

Abbreviations: **APO**=Greatest anteroposterior length taken along the midline of the occlusal surface of the tooth; **AT**=Greatest transverse width of the trigon/trigonid cusps; **PT**=Greatest transverse width of the talon/talonid cusps; **HT**=Greatest transverse width of the hypoconulid complex. Dental nomenclature (B-E) is modified from Wright (1989, 1991, 1998) in regards to the posterior heel of upper and lower m3. This accessory cusp-bearing, posteriorly-oriented extension of the M3 and m3's talon/talonid is not referred to in a unified manner within the literature but is typically referred to as the "posterior lobe", "posterior heel", or "heel" (Matthew, 1924; Kinsey, 1974; Schultz & Martin, 1975; Dalquest & Mooser, 1980; Wright & Webb, 1984; Wright, 1989, 1991). Despite indicating a general location on the M3/m3, these terms are undescriptive as they do little to describe the composition of the feature, which bears the hypoconule/hypoconulid and a variable number of accessory cusps. Consequently, the terms hypoconule complex and hypoconulid complex are used herein to better describe both the placement and composition of this feature on the upper and lower dentition, respectively. General morphology of the hypoconulid complex is provided (D) for *Prosthennops serus* (left) and *Mylohus elmorei* (right), however, it should be indicated that there is notable inter- and intraspecific variation in the number of accessory cuspules on the hypoconulid complex.

(A)

APO · APO

HT · PT · AT

(B)
Lower Dentition except m3

Protoconid (pd)
Metaconid (md)
Entoconulid (ed)
Hypoconid (hd)
Entoconid (entd)
Hypoconulid (hyd)

(C)
Upper Dentition except M3

Paraconule (Pae)
Paracone (Pa)
Protocone (Pr)
Metacone (M)
Metaconule (Me)
Hypoconule (Hye)
Hypocone (Hy)

Anterior
Labial ⬌ Lingual
Posterior

(D)
m3

pd · md
entd
hd · ed
hyd
Hypoconulid Complex

pd · md
entd
hd · ed
hyd

(E)
M3

Pae
Pa
Pr
Me
M
Hy
Hye
Hypoconule Complex

Figure 4

Gray Fossil Site tayassuid material assigned to *Mylohyus elmorei*, ETMNH 8046.

This partial cranium exhibits an intact left canine alveolus and right and left P2-M3. Views: A) Lateral; B) occlusal; C) medial. Image is in grayscale to prevent morphologies from being obscured due to coloration.

(A)

30 mm

(B)

(C)
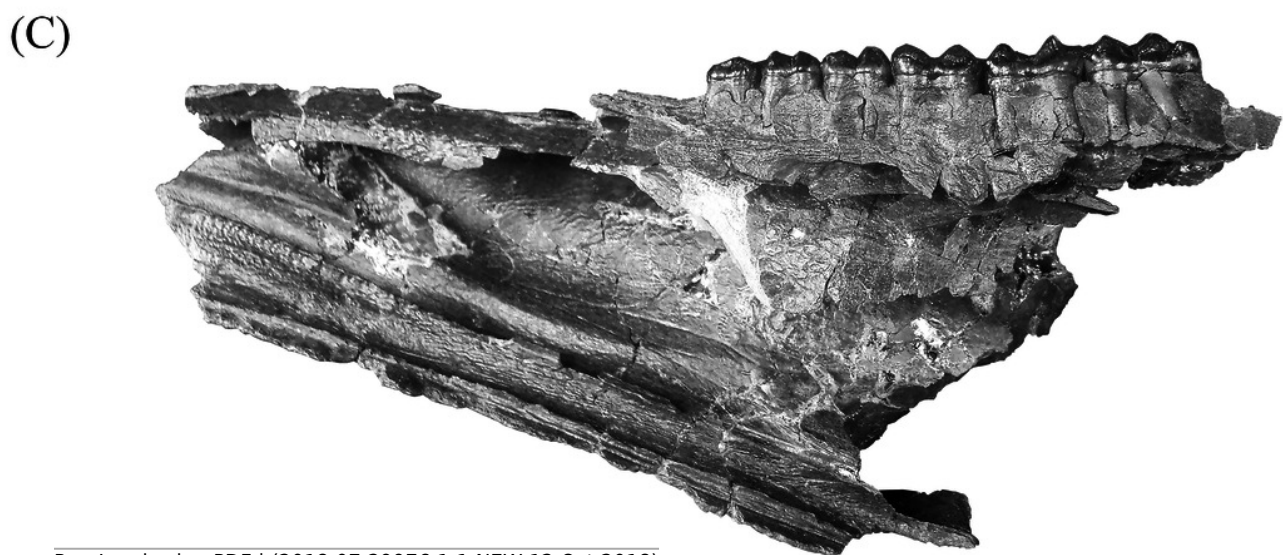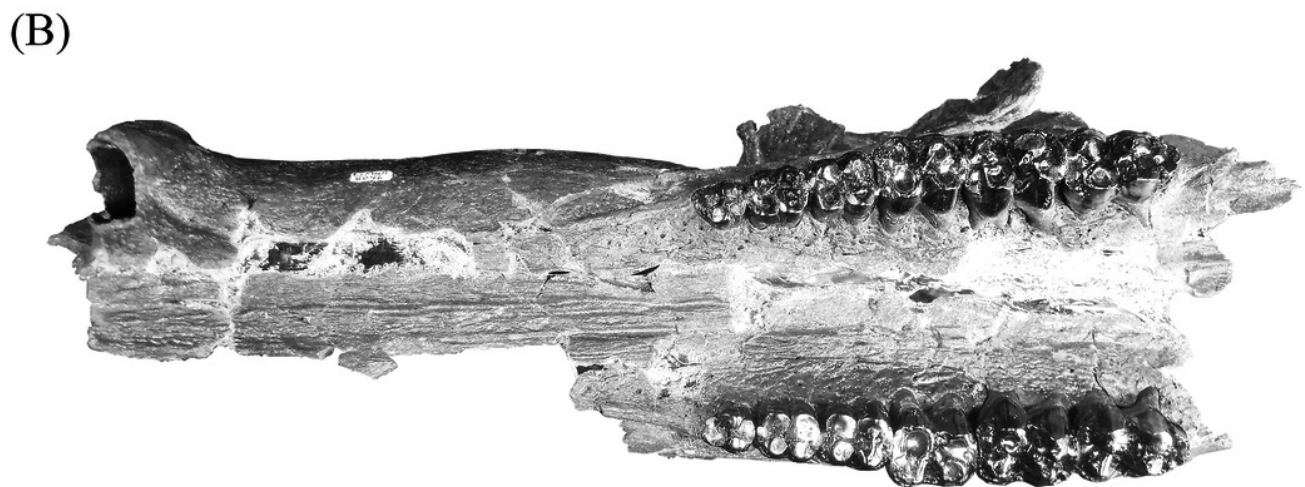
Figure 5

Lateral (A) and buccal (B) view of mandible, ETMNH 8046, of *Mylohyus elmorei* bearing right p2-m3 and left p3-m3.

Image is in grayscale to prevent morphologies from being obscured due to coloration.
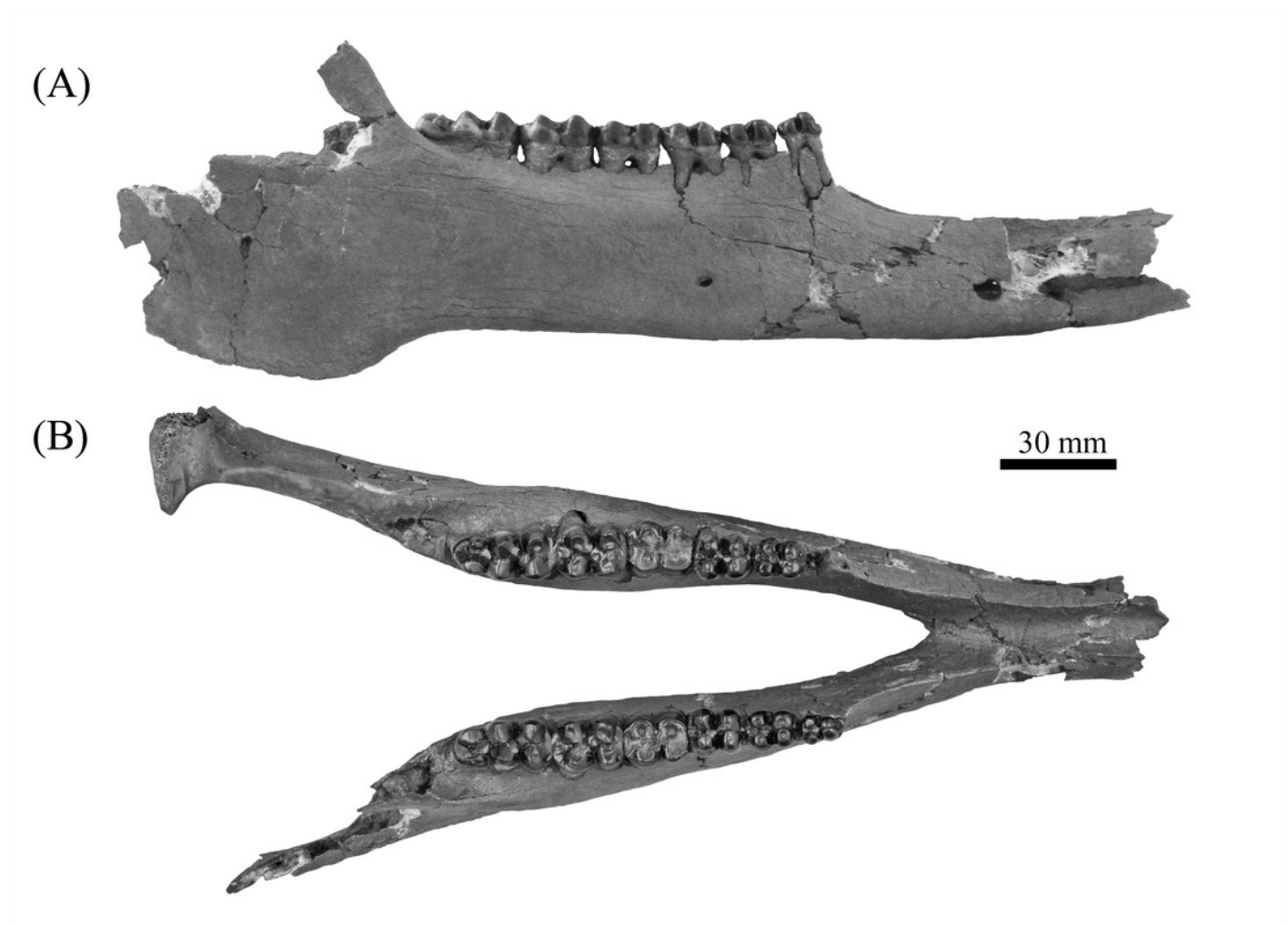
Figure 6

Upper dentitions of Gray Fossil Site and Palmetto Fauna *Mylohyus elmorei*.

Specimens observed include UF/TRO 440 (A), UF 203540 (B), UF 12265 (C), ETMNH 8046 (D), and ETMNH 7279 (E). Image is in grayscale to prevent morphologies from being obscured due to coloration.
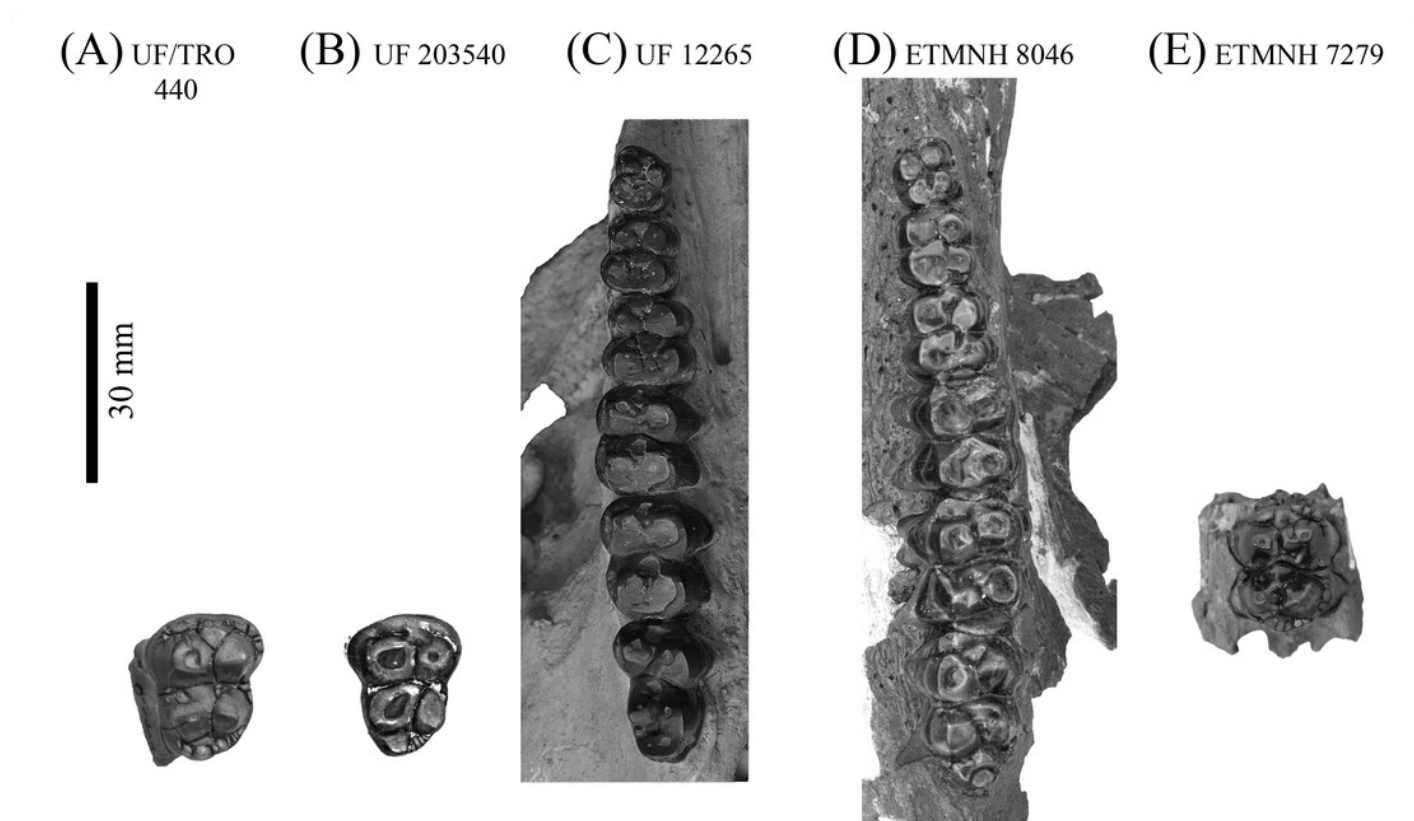
Figure 7

Lower dentition of *Mylohyus elmorei*.

Observed specimens are ETMNH 17219 (A), ETMNH 19281 (B), ETMNH 8046 (C), UF/TRO 412 (D), and UF 294749 (E). Image is in grayscale to prevent morphologies from being obscured due to coloration.
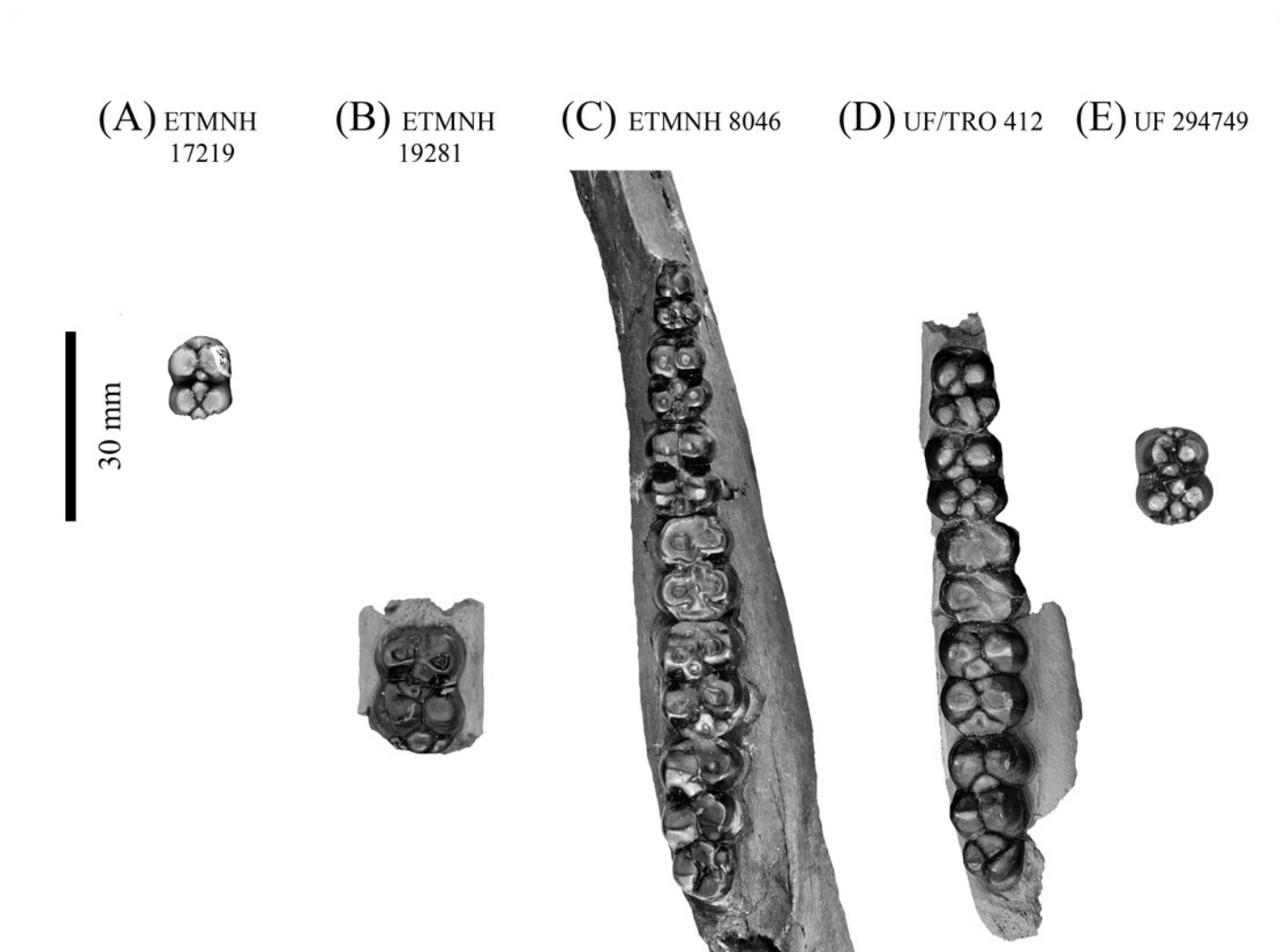
Figure 8

Partial crania, ETMNH 8046 (A) and UF 12265 (B), of *Mylohyus elmorei* in occlusal view.

Image is in grayscale to prevent morphologies from being obscured due to coloration.
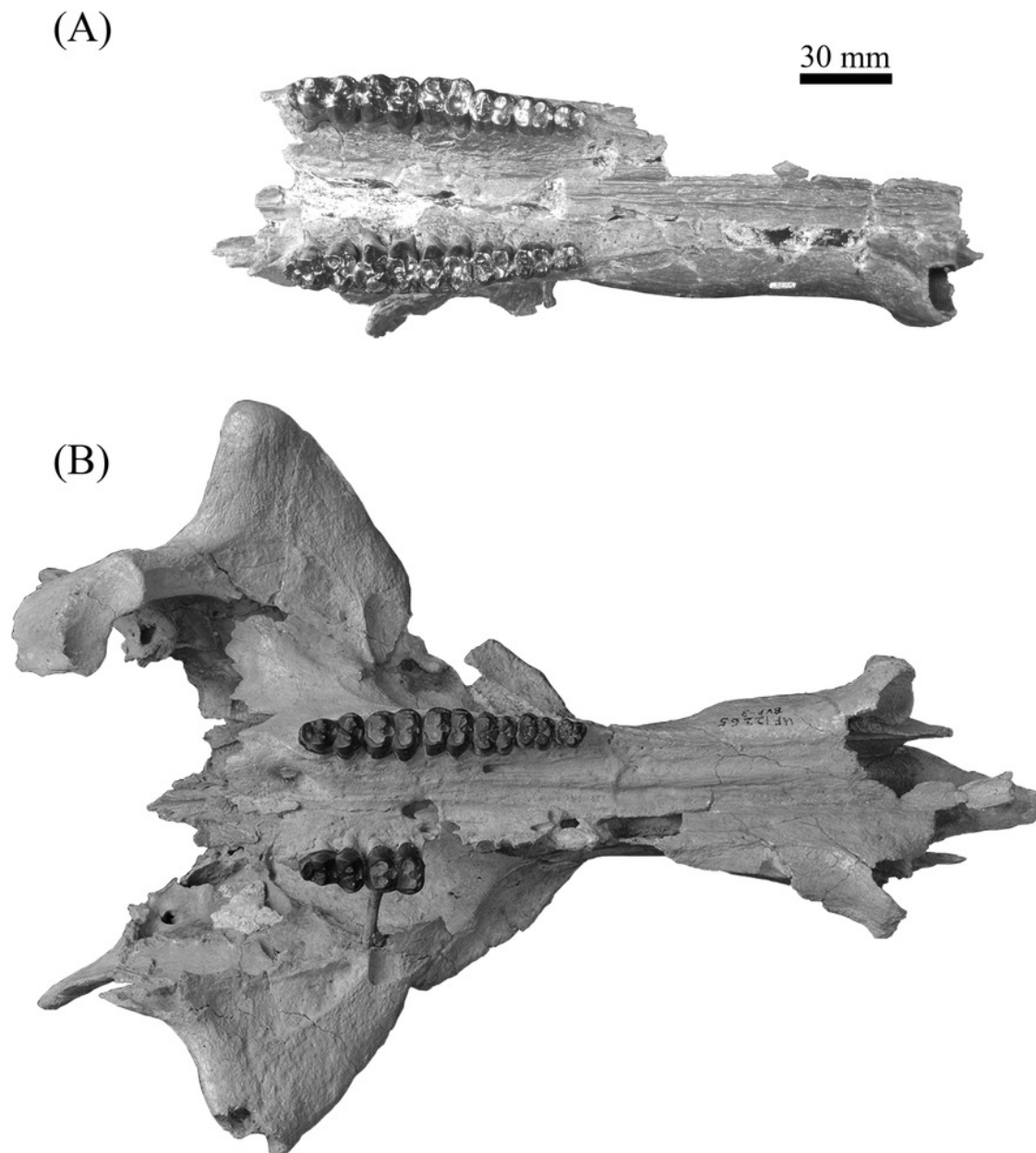
Figure 9

Partial crania, ETMNH 8046 (A) and UF 12265 (B), of *Mylohyus elmorei* in dorsal view.

Image is in grayscale to prevent morphologies from being obscured due to coloration.
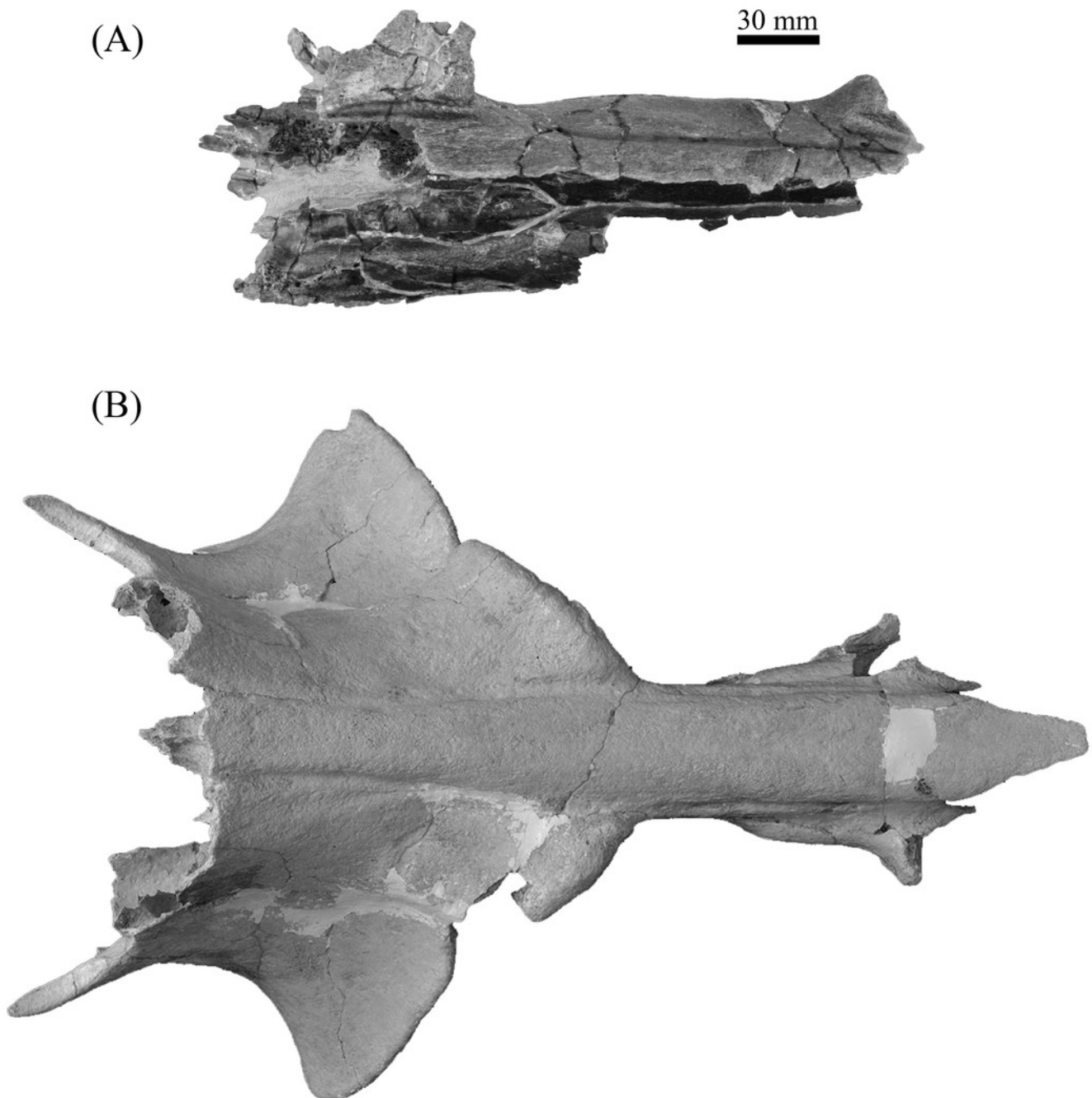
Figure 10

Comparison of partial *Prosthennops* cf. *P. serus* and *Prosthennops serus* mandibles, UF 212306 (A and C) and ETMNH 5615 (B and D), respectively.

Image is in grayscale to prevent morphologies from being obscured due to coloration.
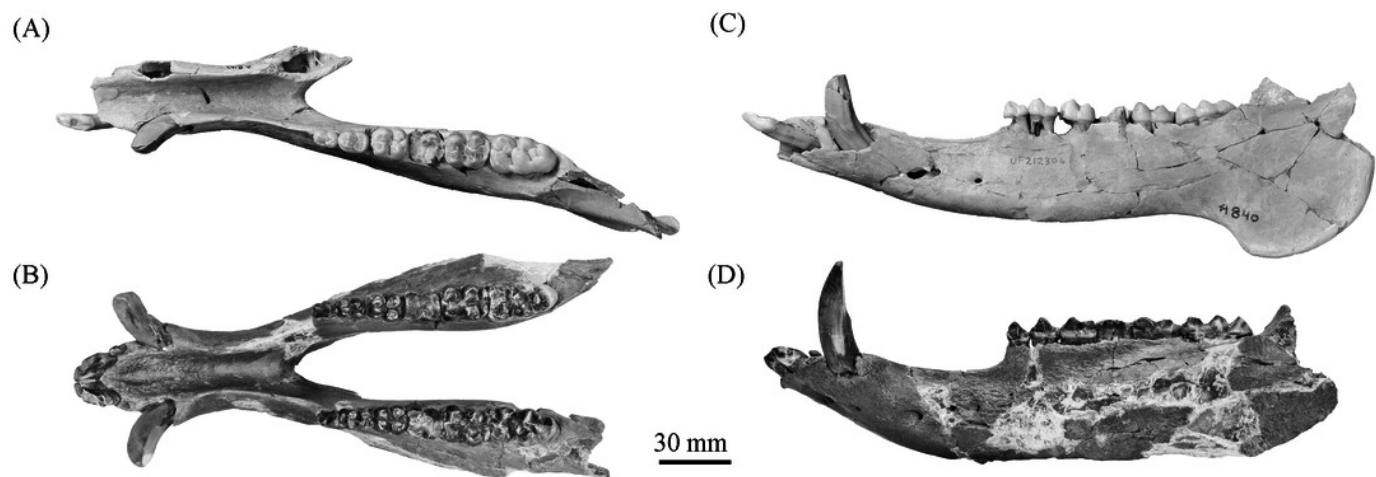
Figure 11

Comparison of lower dentition of *Prosthennops serus* and *Prosthennops* cf. *P. serus*.

Observed specimens: ETMNH 5615 (A), UF/TRO 413 (B), UF 212306 (C), and UF 220251 (D). Image is in grayscale to prevent morphologies from being obscured due to coloration.